European Journal of Medicinal Chemistry 222 (2021) 113592

Contents lists available at ScienceDirect

European Journal of Medicinal Chemistry

journal homepage: http://www.elsevier.com/locate/ejmech

Research paper

5-Aminonaphthalene derivatives as selective nonnucleoside nuclear receptor binding SET domain-protein 2 (NSD2) inhibitors for the treatment of multiple myeloma

Shuni Wang [a, b, 1], Hong Yang [a, b, 1], Mingbo Su [c, 1], Fulin Lian [a, b], Zhanqing Cong [a, b], Rongrui Wei [a, b], Yubo Zhou [a, b, d], Xingjun Li [a, b], Xingling Zheng [a, b], Chunpu Li [a, b, e], Xuhong Fu [a, b], Xu Han [a, b], Qiongyu Shi [a, b], Cong Li [a, b], Naixia Zhang [a, b], Meiyu Geng [a, b], Hong Liu [a, b, c, e], Jia Li [a, b, c, d, e, **], Xun Huang [a, b, e, ***], Jiang Wang [a, b, e, *]

[a] State Key Laboratory of Drug Research and CAS Key Laboratory of Receptor Research, Shanghai Institute of Materia Medica, Chinese Academy of Sciences, 555 Zu Chong Zhi Road, Shanghai, 201203, China
[b] University of Chinese Academy of Sciences, No.19A Yuquan Road, Beijing, 100049, China
[c] School of Chinese Materia Medica, Nanjing University of Chinese Medicine, Qixia District, Nanjing, 210023, China
[d] Zhongshan Institute of Drug Discovery, Institution for Drug Discovery Innovation, Chinese Academy of Science, Zhongshan, 528400, China
[e] School of Pharmaceutical Science and Technology, Hangzhou Institute for Advanced Study, UCAS, Hangzhou, 310024, China

ARTICLE INFO

Article history:
Received 20 January 2021
Received in revised form
19 May 2021
Accepted 27 May 2021
Available online 5 June 2021

Keywords:
NSD2
Methyltransferase
HTS
Multiple myeloma
5-Aminonaphthalene derivatives
Inhibitor

ABSTRACT

Approximately 20% of multiple myeloma (MM) are caused by a chromosomal translocation t (4; 14) that leads to the overexpression of the nuclear receptor binding SET domain-protein 2 (NSD2) histone methyltransferase. NSD2 catalyzes the methylation of lysine 36 on histone H3 (H3K36me2) and is associated with transcriptionally active regions. Using high-throughput screening (HTS) with biological analyses, a series of 5-aminonaphthalene derivatives were designed and synthesized as novel NSD2 inhibitors. Among all the prepared compounds, **9c** displayed a good NSD2 inhibitory activity (IC_{50} = 2.7 μM) and selectivity against both SET-domain-containing and non-SET-domain-containing methyltransferases. Preliminary research indicates the inhibition mechanism of compound **9c** by significantly suppressed the methylation of H3K36me2. Compound **9c** specifically inhibits the proliferation of the human B cell precursor leukemia cell line RS4:11 and the human myeloma cell line KMS11 by inducing cell cycle arrest and apoptosis with little cytotoxicity. It has been reported that the anti-cancer effect of compound **9c** is partly achieved by completely suppressing the transcriptional activation of NSD2-targeted genes. When administered intraperitoneally at 25 mg/kg, compound **9c** suppressed the tumor growth of RS4:11 xenografts *in vivo* and no body weight loss was detected in the tested SCID mice.

1. Introduction

Nuclear receptor binding SET domain-protein 2 (NSD2) is known as multiple myeloma SET domain (MMSET) or Wolf–Hirschhorn syndrome candidate 1 (WHSC1), which has the lowest molecular weight among the NSD family [1–3]. An increasing amount of evidence has shown that NSD2 is involved in cancer pathogenesis. The overexpression of NSD2 is associated with higher grades of bladder, oligodendroglioma, breast, prostate, head and neck, and liver cancers. Previous research has shown a clear role of NSD2 in the oncogenetic process among multiple myeloma (MM) and acute lymphoblastic leukemia (ALL) cancer types. The t (4; 14) (p16; q32) translocation is observed in approximately 20% of

* Corresponding author. State Key Laboratory of Drug Research and CAS Key Laboratory of Receptor Research, Shanghai Institute of Materia Medica, Chinese Academy of Sciences, 555 Zu Chong Zhi Road, Shanghai, 201203, China.
** Corresponding author. State Key Laboratory of Drug Research and CAS Key Laboratory of Receptor Research, Shanghai Institute of Materia Medica, Chinese Academy of Sciences, 555 Zu Chong Zhi Road, Shanghai, 201203, China.
*** Corresponding author. State Key Laboratory of Drug Research and CAS Key Laboratory of Receptor Research, Shanghai Institute of Materia Medica, Chinese Academy of Sciences, 555 Zu Chong Zhi Road, Shanghai, 201203, China.
E-mail addresses: jli@simm.ac.cn (J. Li), xhuang@simm.ac.cn (X. Huang), jwang@simm.ac.cn (J. Wang).
[1] These authors contributed equally to this study.

https://doi.org/10.1016/j.ejmech.2021.113592
0223-5234/

MM, which is the second most frequent translocation observed in this disease, and closely associated with poor prognosis. This translocation results in the overexpression of both NSD2 and fibroblast growth factor receptor 3 (FGFR3); however, approximately 30% of MM patients only overexpress the NSD2 gene, suggesting its pivotal role in the progression of the disease. NSD2 knockdown leads to apoptosis, while overexpression of NSD2 can induce oncogenic transformation [4–7]. A number of ALLs bearing a point lysine mutation (E1099K) in the cleft between the SET and post-SET domains of NSD2 have demonstrated an enhanced methyltransferase activity of NSD2. Genes involved in epithelial to mesenchymal transition (EMT), embryonic development, cell cycle regulation and microtubule disassembly were found to be significantly upregulated in the E1099K NSD2 cell lines [8].

As a member of histone lysine methyltransferase (HKMT) family, NSD2 methylates lysine 36 of histone H3 (H3K36), which is responsible for the transcription activation of a number of genes [9–13]. Abnormal methylation at H3K36 has been widely implicated in a variety of cancers, including MM harboring the translocation t (4; 14) and ALL bearing the E1099K mutation [14–17]. In these cancers, the accumulation of H3K36 methylation is frequently observed and associated with oncogenic programming, including dysregulation of genes related to cell death, EMT, cell cycle regulation and DNA repair. Therefore, the enzymes involved in post-translational modification are regarded as potential targets in drug discovery.

To date, few selective nucleoside and nonnucleoside NSD2 inhibitors have been reported. *S*-Adenosyl-L-homocysteine (**1,** SAH) is a nucleoside NSD2 inhibitor with low inhibitory activity (54% @ 30 μM). Heightman et al. reported that the antifungal drug sinefungin (**2**) exhibited weak NSD2 inhibitory activity (IC_{50} = 26 ± 4.5 μM), and *N*-alkyl derivatization of sinefungin yielded the best compound in this series, **3**, which showed good binding affinity (K_d = 1.6 μM) and inhibitory effect at micromolar level (IC_{50} = 3.3 ± 1.0 μM), making compound **3** more potent than SAH (**1**) (Fig. 1) [18]. In addition to nucleoside NSD2 inhibitors, several nonnucleoside NSD2 inhibitors (**4**–**7**) have been reported by Luccio and coworkers [19–21]. Although these compounds exhibited impressive NSD2 inhibitory activities at micromolar level, their selectivities to the other members of the NSD family are not satisfactory. Besides, the knowledge of structural modifications are not sufficiently comprehensive for the evaluation of the structure-activity relationship (SAR) and the key pharmacophores (Fig. 1). Therefore, the discovery and development of potent nonnucleoside NSD2 inhibitors based on detailed SAR studies is still of great interest.

In this study, high-throughput screening (HTS) was applied to discover novel NSD2 inhibitors. A series of 5-aminonaphthalene derivatives were designed, synthesized, and biologically evaluated as novel selective NSD2 inhibitors. Further studies demonstrated that the most potent compound, **9c**, significantly inhibited cancer cell proliferation. Taken together, the results indicate that compound **9c** and its analogs are new potential NSD2-specific inhibitors, and provide us with new structural information for developing more potent NSD2 inhibitors.

2. Results and discussion

2.1. Design of 5-aminonaphthalene derivatives

To develop a new structural class of potent NSD2 inhibitors, we used HTS to identify small molecules that can inhibit NSD2. A total of 296 080 compounds from the Chinese National Compound Library were screened. We obtained 26 compounds as hits from the screening at a concentration of 20 μg/mL, with the hit rate of 0.087‰. Among them, compound **8**, which potently inhibited NSD2 (IC_{50} = 19.4 ± 6.5 μM), was identified through HTS. To find out more potent inhibitors, we focused our design attempts on the aminonaphthalene scaffold. In an initial effort to enhance the inhibitory activity against NSD2, our first round of analogs (**9a-9b**) were designed by installing different bicyclic aromatic moieties in compound **8**. In addition, the replacement of the amide moiety in compound **8** with a sulfamide yielded compound **9c**. Next, compounds **10a-10d** were designed to explore the influence of the position of the substituent (the amino and sulfamide moieties) on the naphthalene scaffold based on compound **9c**. Finally, a series of 5-aminonaphthalene-1-sulfonamides (**11a-11ac**) were designed to systematically investigate the SAR involving the R^1 and R^2 substituents (Fig. 2).

2.2. Chemistry

Four synthetic routes were designed to obtain desired compounds **8**–**11** (Schemes 1–4). Condensation of carboxylic acid **12** and benzylamine yielded the desired compounds **9a**-**9b**. Compound **8** was obtained after salification with hydrochloric acid (Scheme 1). As shown in Scheme 2, naphthalene sulfonic acids **15** with amino substituents at different positions were acetylated with acetyl chloride to afford sulfonic acids **16**, which were converted to corresponding sulfonyl chlorides **17** by treatment with phosphorus pentachloride. Then, compounds **17** were coupled with amines **18** to provide compounds **11t** and **19**. Desired compounds **9c**, **10a**-**10d** and **11a**-**11q** were generated by hydrolysis of intermediates **11t** and **19**. Compounds **11r**-**11s** could be easily prepared *via* a coupling reaction of commercially available naphthalene sulfonyl chloride **20** and benzylamine followed by salification with HCl (Scheme 3). As shown in Scheme 4, compound **9c** underwent reductive amination with aldehyde or ketones **21** and was subsequently salified with HCl to afford desired compounds **11u**-**11ac**.

2.3. Structure-activity relationship of 5-aminonaphthalene derivatives

With the hit compound **8** in hand, the scaffold was firstly investigated. As shown in Table 1, replacement of the aminonaphthalene scaffold in compound **8** with an indole afforded compound **9a**, which has almost no NSD2 inhibitory activity at 20 μM, and with a quinolone afforded compound **9b**, which showed activity comparable to hit compound **8**. To our delight, when the amide moiety in compound **8** was replaced with a sulfamide, the resulting 5-aminonaphthalene-1-sulfonamide derivative **9c** displayed a 7-fold improvement in inhibitory potency. Then, we explored the influence of the position of the substituents (the amino and sulfamide groups) on the naphthalene core (**10a**-**10d**) (Table 1). Compared with compound **9c**, altering the positions of the amino and sulfamide moieties did not enhance the NSD2 inhibitory activity (IC_{50} > 20 μM).

According to the results above, we selected compound **9c** as the lead compound and systematically investigated the SAR of substituents R^1 and R^2 on the 5-aminonaphthalene-1-sulfonamide scaffold (Tables 2 and 3). First, compounds **11a**-**11q** with different R^1 groups were designed to further enhance the activity. Interestingly, compared with compound **9c**, which possesses a benzyl group (R^1), compounds with phenyl (**11a**) or phenethyl (**11b**) substituents displayed decreased activity. Further introduction of a halogen (**11c**), an electron-donating (**11d**) or an electron-withdrawing (**11e**-**11h**) substituent at the *para*- or *meta*-position of the benzyl group resulted in a significant decrease in potency. The replacement of the phenyl group in compound **9c** with heteroaromatic groups, such as pyridyl (**11i**) or thienyl (**11j**), leads to a

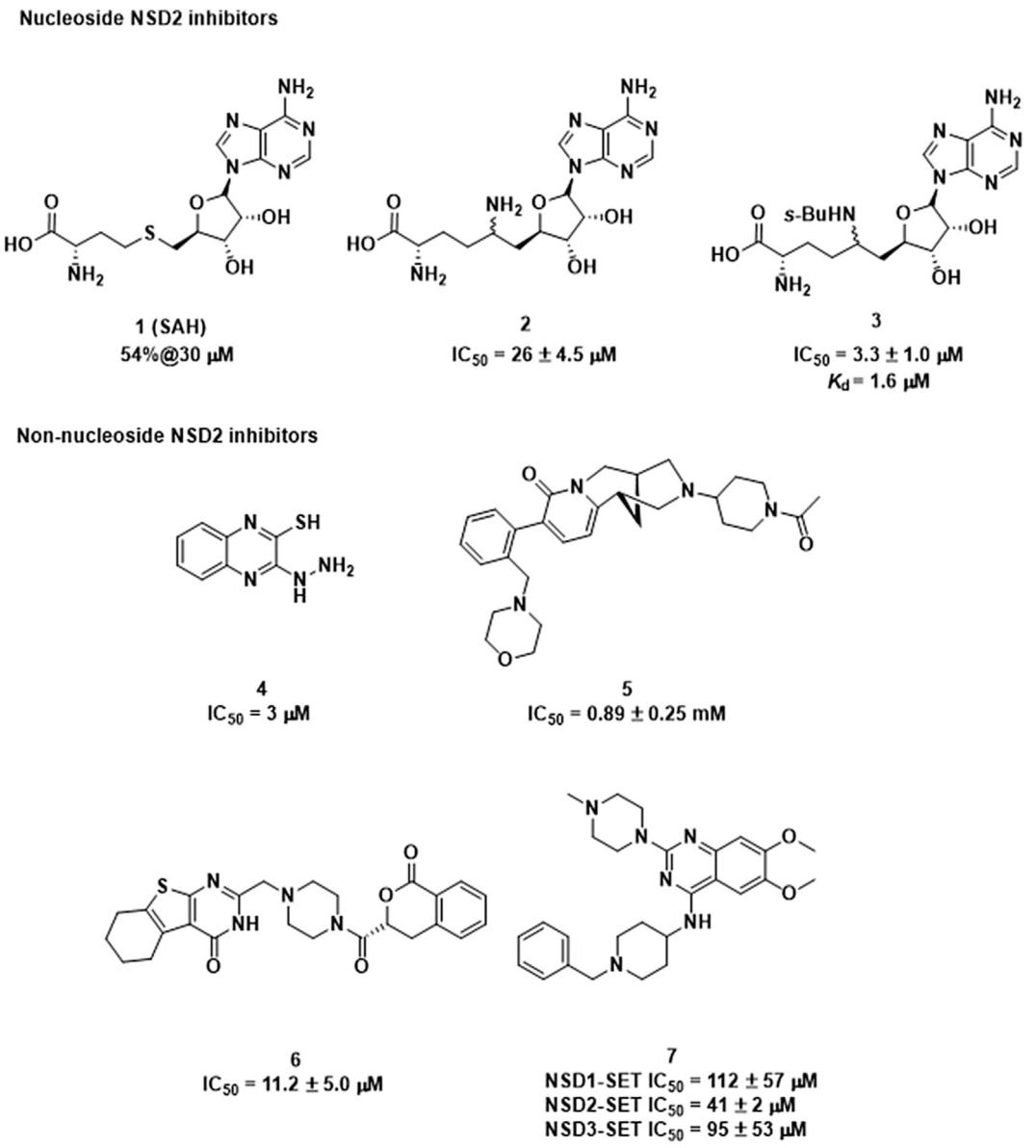

Fig. 1. Reported nucleoside and nonnucleoside NSD2 inhibitors.

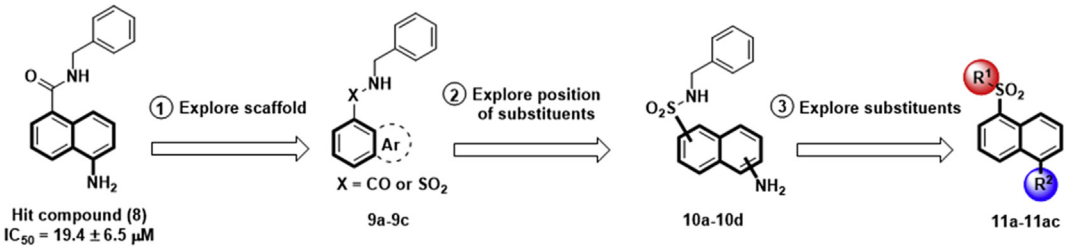

Fig. 2. Design of 5-aminonaphthalene derivatives as novel NSD2 inhibitors.

decreased inhibitory activity against NSD2 (IC_{50} > 20 μM). In addition, when the phenyl group was replaced with aliphatic moieties, such as cyclohexyl (**11k**) or piperidyl (**11l**), reduced activities were observed (IC_{50} > 20 μM). Interestingly, NSD2 inhibitor **11m**, bearing a 1-methylpiperidinyl unit in place of the phenyl moiety, exhibited potency comparable to compound **9c**. The introduction of bulky 2-phenylcyclopropyl (**11n**) or *tert*-butyl groups (**11o**), on the contrary, resulted in lower potencies compared to compound **9c**. Finally, removing the hydrogen atom from the sulfamide moiety (**11p**-**11q**) resulted in substantial losses in NSD2 inhibitory activity. These results indicated that the hydrogen of the sulfamide is probably a key hydrogen bond donor

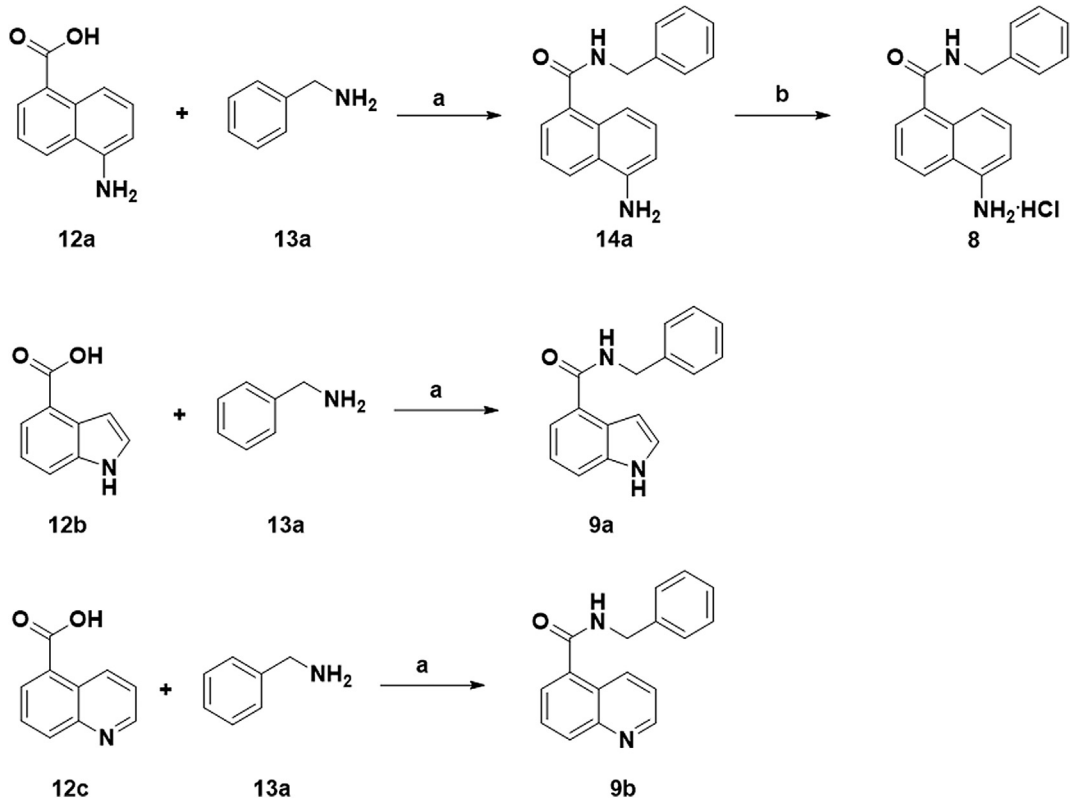

Scheme 1. Synthetic route to desired compounds **8** and **9a-9b**[a].
[a]Reaction conditions and reagents: (a) HOBt, EDCI, Et_3N, DCM, 0 °C to r.t., 8 h; (b) 4 *N* HCl in dioxane, 2 h.

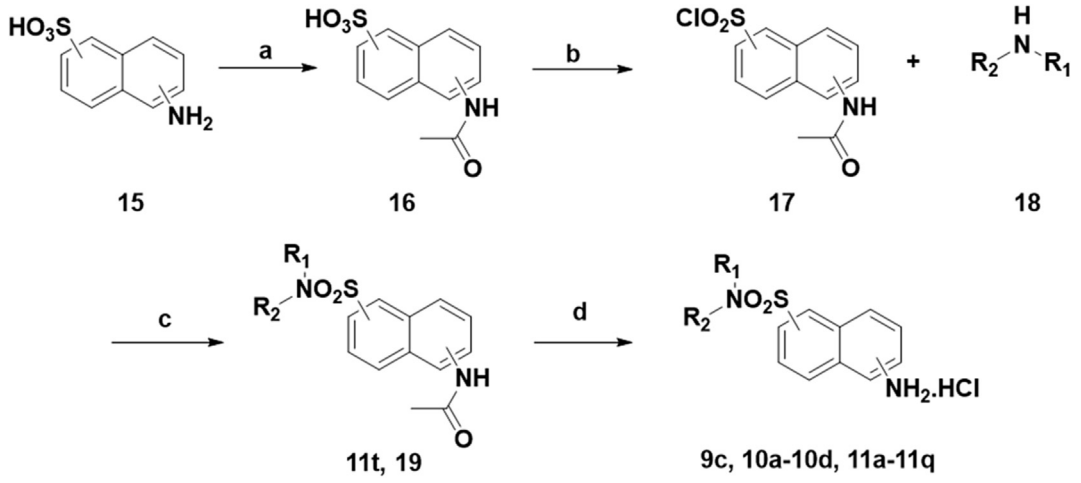

Scheme 2. Synthetic routes to compounds **9c**, **10a-10d**, **11a-11q**, and **11t**[a].
[a]Reaction conditions and reagents: (a) acetyl chloride, Et_3N, DCM, 0 °C to r.t., 8 h; (b) PCl_5, DCM, 40 °C, 4 h; (c) amines, Et_3N, CH_3CN, r.t., 5 h; (d) 6 *N* HCl, EtOH, reflux, 12 h.

and it forms a hydrogen bond with an amino acid residue in the binding pocket of NSD2.

Next, we focused on the SAR of the R^2 group and evaluated the NSD2 inhibitory activity of the candidate compounds **11r**-**11ac** (Table 3). First, we removed the amino group from compound **9c** to afford compound **11r**, which showed significantly lower potency. This result demonstrated that the amino group at the 5-position of the naphthalene is pivotal for the inhibitory activity of the compound. When R^2 was a dimethylamino or an acetamino group, the corresponding compounds, **11s** and **11t**, showed no activity against NSD2 (IC_{50} > 20 μM). Based on the aforementioned results, we alkylated the amino acids to further enhance the potency. However, the introduction of simple alkyl groups (compounds **11u**-**11v**) caused slight decreases in potency. When introducing a piperidyl moiety to the amino group, synthesized compound **11w** showed moderate inhibitory activity against NSD2. Further alkylation of the piperidyl (**11x** and **11y**) could enhance or maintain the potency, and compound **11y**, with an *N*-ethyl-substituted piperidyl moiety, exhibited comparative good activity against NSD2 with an IC_{50} less than 5 μM. *N*-Acetyl-substituted piperidyl compound **11z** also

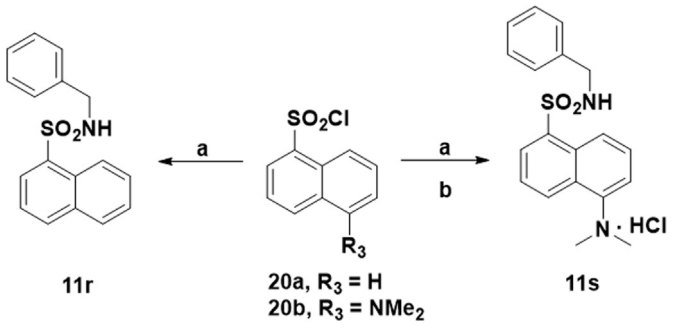

Scheme 3. Synthetic routes to compounds **11r-11s**[a].
[a]Reaction conditions and reagents: (a) benzylamine, Et_3N, CH_3CN, r.t., 5 h; (b) 4 *N* HCl in dioxane, 2 h.

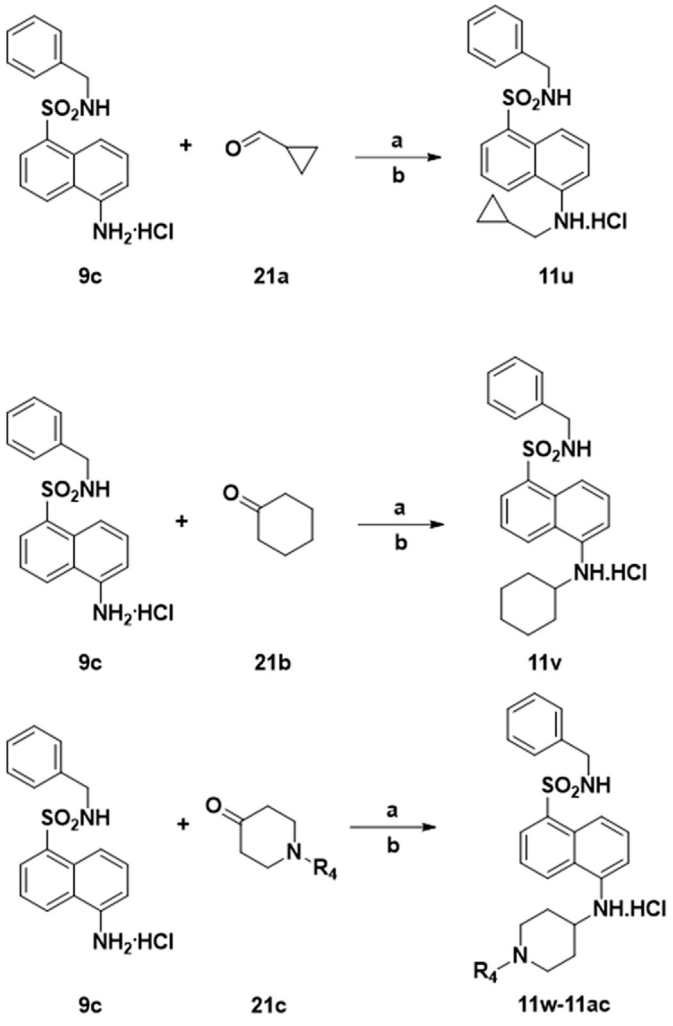

Scheme 4. Synthetic routes to compounds **11u-11ac**[a].
[a]Reaction conditions and reagents: (a) Et_3N, AcOH, $NaBH_3CN$, r.t., 12 h; (b) 4 *N* HCl in dioxane, 2 h.

showed good activity with an IC_{50} less than 10 μM. However, compounds with bulkier substituents, such as benzoyl (**11aa**) and carbobenzyloxy (**11 ab**), displayed significantly lower inhibitory activities against NSD2. Finally, the introduction of a methylsulfonyl unit to the piperidyl moiety afforded compound **11ac**, which showed moderate activity against NSD2. These results indicated

Table 1
SAR of scaffold and position of the substituents on the naphthalene [a].

Compd.	Structure	IC_{50} (μM)	Compd.	Structure	IC_{50} (μM)
8	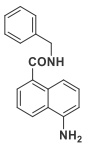	19.4 ± 6.5	**10a**	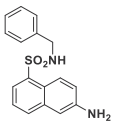	>20
9a	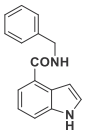	>20	**10b**	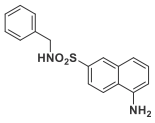	>20
9b	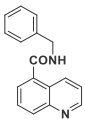	19.6 ± 6.5	**10c**	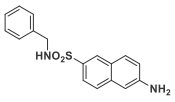	>20
9c	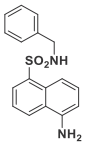	2.7 ± 0.3	**10d**	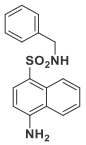	>20
SAH	–	39.1 ± 4.1			

[a] IC_{50} values are reported as the mean ± SD deviations, n ≥ 3.

that at least one active hydrogen atom of the amino group must be reserved, which probably forms a key hydrogen bond with NSD2.

2.4. Compound *9c* interacts with NSD2

Base on the enzymatic inhibitory potency against NSD2, we selected compound **9c** as the representation to further confirm whether these 5-aminonaphthalene derivatives as NSD2 inhibitors could assuredly interact with the protein through NMR analysis. And ligand observed CPMG and STD NMR experiments were performed. In consistent with the result from the enzymatic inhibitory assay, strong binding effects were clearly observed in both ligand observed STD (Fig. 3A) and CPMG NMR spectra (Fig. 3B), which indicating an interaction between compound **9c** and NSD2.

2.5. Compound *9c* selective against NSD2

Based on the NSD2 inhibitory activity, compound **9c** was selected for evaluation of its specificity for NSD2. The inhibitory activity of compound **9c** was examined against mutant NSD2 (E1099K), NSD1, SETD2, EZH2, MLL1, MLL4, DOT1L, PRMT4, and PRMT5 (Table 4). As depicted in Table 4, compound **9c** exhibited remarkable selectivity against NSD2 over other human methyltransferases, including both SET-domain-containing (NSD1, SETD2, EZH2, MLL1, and MLL4) and non-SET domain-containing methyltransferases (DOT1L, PRMT4, and PRMT5).

2.6. Analysis of H3K36me2 levels in RS4:11 and KMS11 cell lines by western blotting

Next, compound **9c** was examined for its effects on the levels of H3K36me2. As shown in Fig. 4, Western blot analysis revealed that compound **9c** significantly suppressed the methylation of H3K36me2 in a dose-dependent manner in RS4:11, MV4;11, KMS11, and OPM-2 cell lines (Fig. 4A). Further analyses demonstrated that the inhibition of H3K36me2 is highly selective relative to other

Table 2
SAR of substituent R^1 on the 5-aminonaphthalene-1-sulfonamide scaffold [a].

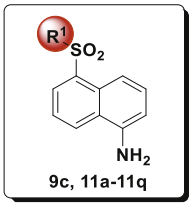

Compd.	R^1	IC_{50} (μM)	Compd.	R^1	IC_{50} (μM)
9c		2.7 ± 0.3	**11i**	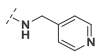	26.0 ± 2.4
11a		>20	**11j**	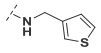	22.7 ± 7.9
11b	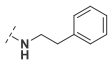	15.4 ± 6.1	**11k**	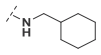	>20
11c	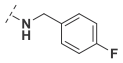	14.1 ± 11.6	**11l**	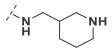	>20
11d	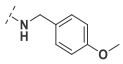	13.5 ± 2.1	**11m**	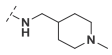	3.4 ± 0.4
11e	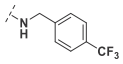	10.4 ± 1.5	**11n**	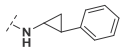	19.9 ± 4.4
11f	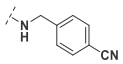	18.1 ± 4.4	**11o**		18.4 ± 6.3
11g	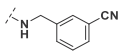	>20	**11p**	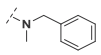	>20
11h	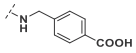	>20	**11q**	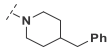	>20
SAH		39.1 ± 4.1			

[a] IC_{50} values are reported as the mean ± SD deviations, n ≥ 3.

Table 3
SAR of substituent R^2 on the 5-aminonaphthalene-1-sulfonamide scaffold[a].

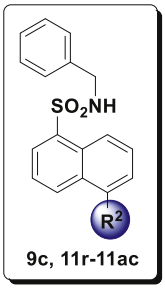

Compd.	R^2	IC_{50} (μM)	Compd.	R^2	IC_{50} (μM)
9c	$-NH_2$	2.7 ± 0.3	**11x**		6.0 ± 1.5
11r	H	>20	**11y**	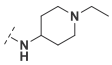	3.2 ± 0.8
11s		>20	**11z**	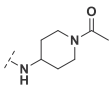	7.5 ± 3.3
11t		>20	**11aa**	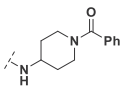	18.0 ± 12.1
11u		10.7 ± 1.6	**11ab**	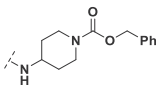	>20
11v		12.6 ± 2.1	**11ac**	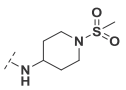	11.8 ± 1.8
11w		10.2 ± 1.3	**SAH**	—	39.1 ± 4.1

[a] IC_{50} values are reported as the mean ± SD deviation, n ≥ 3.

methylated sites (Fig. 4B). Total histone H3 and NSD2 were not affected by compound **9c** (Fig. 4B); thus, the reduction in H3K36me2 is due to the direct inhibition of NSD2 methyltransferase activity rather than the degradation of histone H3 or NSD2.

2.7. Cell-based activity

To determine the antitumor potential of compound **9c**, we evaluated its effects on cell proliferation in a panel of human cell lines, including gastric cancer, hepatic carcinoma, breast cancer, lung cancer, thyroid carcinoma, and hematological tumor cells. These cell lines with different genetic background exhibited various levels of sensitivity to compound **9c**. Based on the sources of the cell lines, compound **9c** showed relatively low IC_{50} values against the hematological tumor cell lines (Fig. 5A). The results also indicated that compound **9c** remarkably inhibited cell proliferation in the ALL cell line RS4:11 and the MM cell line KMS11 with IC_{50} values of 0.52 μM and 1.88 μM, respectively (Fig. 5A). However, a slight proliferative effect was observed in NCI−H929, U2932, HL-60, OCI-AML5, RPMI-8226, Pfeiffer, MV4;11, KARPAS-422, WSUCLDL2, OPM-2, MOLT4, and Jurkat cells.

Due to the remarkable inhibition effect on the growth of the RS4:11 and KMS11 cell lines by compound **9c**, it was further analyzed by using different timing and dosing to investigate its effect on antiproliferation and apoptotic activities in these two most sensitive cell lines. In the RS4:11 and KMS11 cell lines, potent inhibition of cell proliferation was observed for 6 consecutive days, and net decreases in cell number were observed after 2 days. The experiment showed that compound **9c** significantly inhibited the growth rate of RS4:11 and KMS11 cells in a time-dependent and dose-dependent manner (Fig. 5B).

2.8. Compound *9c* induces apoptosis and cell cycle arrest

The effects of compound **9c** on apoptosis and various phases of cell cycle progression were evaluated in RS4:11, KMS11, and MV4;11 cells. RS4:11, KMS11, and MV4;11 cells were treated with vehicle alone or compound **9c** at 5 and 10 μM for 72 h and evaluated by flow cytometry [22]. Compound **9c** induced apoptosis in a dose-dependent manner in the RS4:11 and KMS11 cells. Nevertheless, no pronounced change was observed in the MV4:11 cells (Fig. 6A). According to the subsequent cell cycle analysis, the proportions of RS4:11 cells in the G0/G1 phase of the cell cycle were 47.66% at 5 μM and 60.86% at 10 μM. In contrast, the proportion of untreated cells in the G0/G1 phase of the cell cycle was 41.81%. The proportions of KMS11 cells in the G0/G1 phase of the cell cycle were 44.53% at 5 μM and 45.69% at 10 μM. In contrast, the proportion of untreated cells in the G0/G1 phase of the cell cycle was 32.21% (Fig. 6B). Compared with the control population, the cell cycle data clearly demonstrated that compound **9c** arrested RS4:11 and KMS11 cells

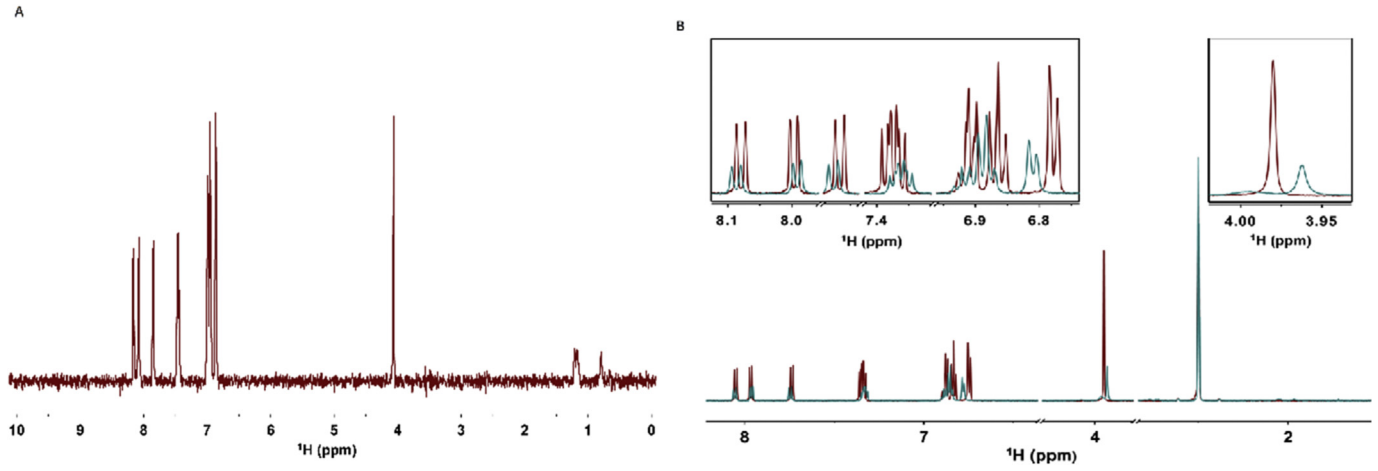

Fig. 3. Ligand observed CPMG and STD spectra confirm that compound **9c** could interact with NSD2. (A) STD spectrum of 200 mM compound **9c** in the presence of 4 mM NSD2. (B) CPMG spectra for 200 mM compound **9c** without (red) or with (cyan) the presence of 4 mM NSD2.

Table 4
Compound **9c** selective against NSD2.[a].

Enzyme	IC_{50} (μM)
NSD2	2.7 ± 0.3
Mutant NSD2 (E1009K)	3.1 ± 0.7
NSD1	>20
SETD2	>20
EZH2	>20
MLL1	>20
MLL4	>20
DOT1L	>20
PRMT4	>20
PRMT5	>20

[a] IC_{50} values are reported the mean ± SD (μM) from two separate experiments.

mainly at the G0/G1 phase. In addition, the G0/G1 fraction in the MV4;11 cells was not significantly increased (Fig. 6B).

*2.9. Compound **9c** suppresses transcriptional activation of NSD2-target genes*

To systematically examine the cellular pathways affected by compound **9c**, we performed RNA sequencing (RNA-seq) on the sensitive cell line RS4:11 by treating the cells with compound **9c** or DMSO as a control for 72 h. By the GO analysis of the RNA-Seq, multiple cellular pathways that are down- or up-regulated have been identified and the top 20 up- and down-regulated genes have been presented between the control group and the treatment group (Fig. 7A and Fig. 7B). According to recent studies [23], genes such as TGFA, MET, PAK1, and RRAS2 were under control of NSD2 mediated H3K36me2. We performed a systematic quantitative direct ChIP analysis comparing H3K36me2 levels in KMS11 cells treated with compound **9c** and DMSO in all regions spanning the four oncogenes (TGFA, PAK1, MET, and RRAS2). The result shows a decreased H3K36me2 signaling in compound **9c-**treated cells compared to DMSO-treated cells (Fig. 7C). These data further support the conclusion that compound **9c** completely suppressed H3K36me2 level in the promoter regions of the NSD2-target genes TGFA, MET, PAK1, and RRAS2 in KMS11 cells.

2.10. In vivo antitumor efficacy and preliminary PK study of compound 9c

Based on its potent effects in cell culture, compound **9c** was selected for evaluation of its *in vivo* antitumor efficacy due to its good inhibitory activity against NSD2. Initially, the pharmacokinetic profiles of compound **9c** were evaluated in CD-1 mice after intraperitoneal (i.p.) at 20 mg/kg and intravenous (i.v.) injection at 2 mg/kg. As shown in Table 5, compound **9c** was suitable for intraperitoneal administration with a satisfactory area under the curve (AUC = 150 h*ng/mL) in CD-1 mice. Then, a RS4:11 xenograft SCID mouse model was prepared according to the procedure described previously [24]. When implanted tumors reached a volume of 100 mm^3, compound **9c** was administered intraperitoneally (i.p.) at 25 mg/kg and 50 mg/kg once a day for 21 consecutive days. Tumor volumes and body weights were monitored over the course of treatment. The tumor growth inhibition (TGI) and relative increment ratio (T/C) were calculated at the end of treatment. As shown in Fig. 8A, treatment with compound **9c** caused a dramatic reduction in tumor growth (25 mg/kg: TGI = 43.6%, T/C = 56.3%; 50 mg/kg: TGI = 37.2%, T/C = 62.8%). Moreover, no body weight loss was detected in the tested SCID mice (Fig. 8B).

3. Conclusions

In summary, a series of 5-aminonaphthalene derivatives were designed, synthesized, and evaluated as novel NSD2 inhibitors for the treatment of cancer. Hit compound **8** was discovered *via* HTS from the compound library, and SAR studies focusing on the scaffold, position of the substituents and types of substituent on the naphthalene core of compound **8** were sequentially conducted. Among the prepared compounds, **9c** displayed the best potency against NSD2 (IC_{50} = 2.7 μM). In our study, we tested the effect of compound **9c** on various histone modifications and found that compound **9c** was able to specifically reduce H3K36me2 level without affecting other histone methylations, such as H3K4me2, H3K27me2 or H3K79me2. Multiple cellular assays demonstrated the anti-tumor effect of compound **9c** *via* proliferation inhibition, $G0/G_1$ arrest, and apoptosis in the human B cell precursor leukemia cell line RS4:11 and the human myeloma cell line KMS11. The RNA sequencing data indicated that compound **9c** completely suppressed the transcriptional activation of the NSD2-target genes TGFA, MET, PAK1, and RRAS2 in KMS11 cells. This scaffold for potent NSD2 inhibitors establishes a new research foundation for the

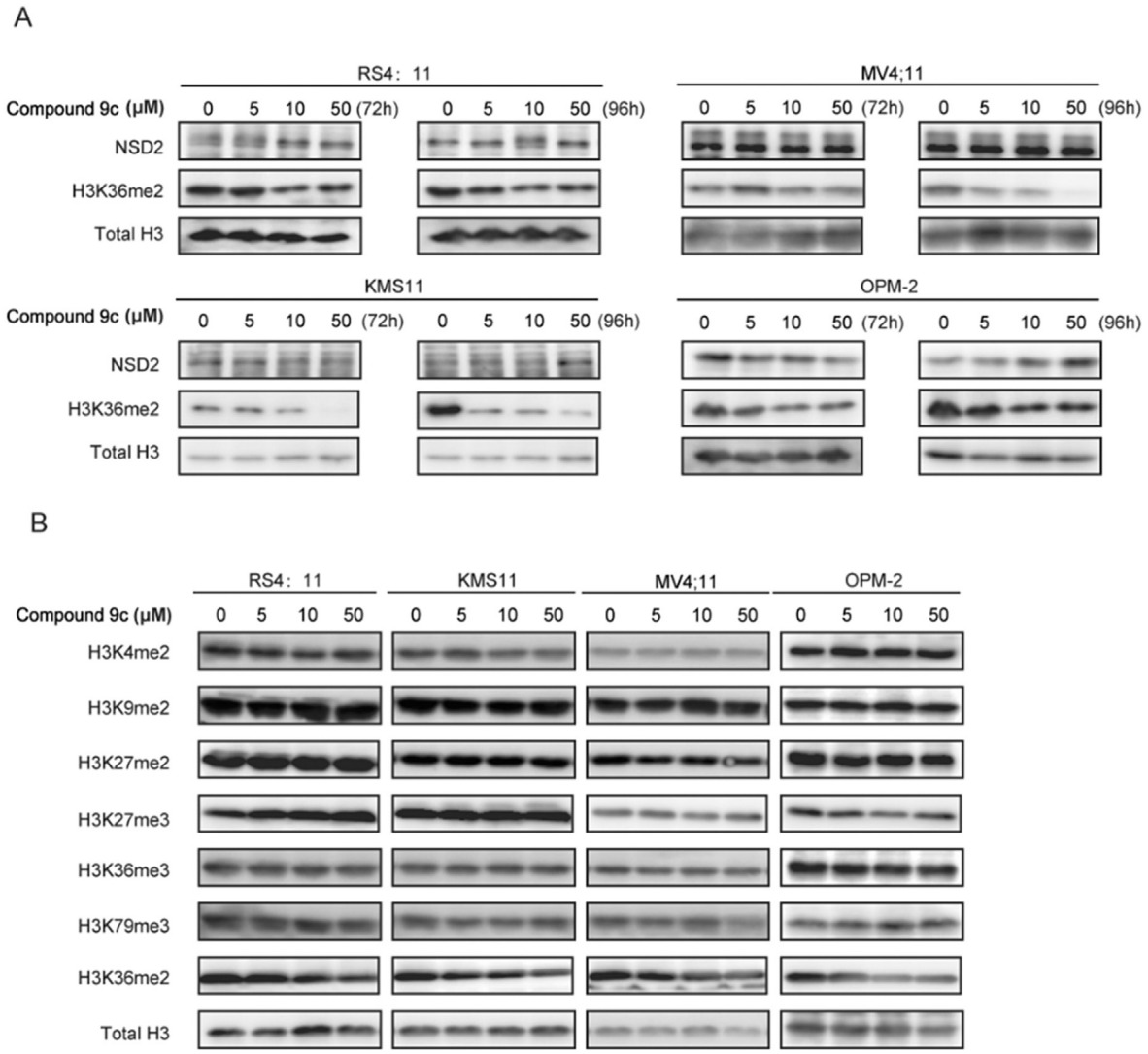

Fig. 4. Cellular mechanistic activity of compound **9c**. (A) RS4:11, MV4;11, KMS11, and OPM-2 cell lines were treated with compound **9c** at the indicated doses and time intervals, and the expressions of NSD2 and H3K36 methylation were profiled. (B) RS4:11, MV4;11, KMS11, and OPM-2 cells lines were treated with compound **9c** (0, 5, 10, and 50 μM) for 4 days, and various histone modifications were detected by western blotting.

discovery of NSD2 small-molecule inhibitors and highlight potentials for the development of new MM agents. We have developed a series of compounds with activity against NSD2, compound **9c** may be useful as a tool molecule, which would require further development and evaluation for treating cancer.

4. Experimental

4.1. Chemistry

The commercially available reagents and chemicals were used without further purification. Nuclear magnetic resonance (NMR) spectroscopy (^{1}H and ^{13}C) spectra was recorded on a Varian-MERCURY Plus-400 MHz, AVANCE III 500 MHz or INVOA-600 MHz instrument. Chemical shifts were reported in parts per million (ppm, δ) downfield from tetramethylsilane. Proton coupling patterns are described as singlet (s), doublet (d), triplet (t), quartet (q), multiplet (m), and broad (br). Low-resolution mass spectra (LRMS) was measured on Agilent Technologies 6120 LC/MS spectrometer. High-resolution mass spectra (HRMS) was measured on Micromass Ultra Q-TOF spectrometer.

4.1.1. 5-Amino-N-benzyl-1-naphthamide hydrochloride (*8*)

To a stirred mixture of commercially available 5-amino-1-naphthoic acid **12a** (250 mg, 1.34 mmol) in anhydrous DCM was successively added EDCI (384 mg, 2.0 mmol), HOBt (270 mg, 2.0 mmol) and triethylamine (278 μL, 2.0 mmol). After 0.5 h, benzylamine (219 μL, 2.0 mmol) was added to the reaction mixture at 0 °C. The reaction mixture was stirred at ambient temperature for 8 h when TLC showed completion of the reaction. The resulting mixture was sequentially washed with water (10 mL x 2), 0.1 *N* HCl (10 mL x 2), 0.1 *N* NaOH (10 mL x 2) and brine (10 mL). The obtained organic solution was concentrated under vacuum and purified by silica gel column chromatography (DCM/MeOH = 100/1) to afford a white solid, which was subsequently dissolved in 4 *N* HCl in dioxane (5 mL) and stirred for 2 h at room temperature. The reaction mixture was concentrated to afford compound **8** as a white solid (320 mg, yield: 86%). Mp 242–244 °C. ^{1}H NMR (400 MHz, DMSO-d_6) δ 9.19 (t, J = 6.1 Hz, 1H), 8.18 (dt, J = 8.2, 1.2 Hz, 1H), 8.08 (dt, J = 8.2, 1.1 Hz, 1H), 7.73 (dd, J = 7.1, 1.4 Hz, 1H), 7.69 (dd, J = 8.3, 7.1 Hz, 1H), 7.61 (dd, J = 7.4, 1.5 Hz, 1H), 7.56 (dd, J = 8.2, 7.4 Hz, 1H), 7.43–7.35 (m, 4H), 7.28 (ddt, J = 7.6, 6.2, 1.8 Hz, 1H), 4.55 (d, J = 6.0 Hz, 2H). ^{13}C NMR (125 MHz, DMSO-d_6) δ 168.31, 139.44,

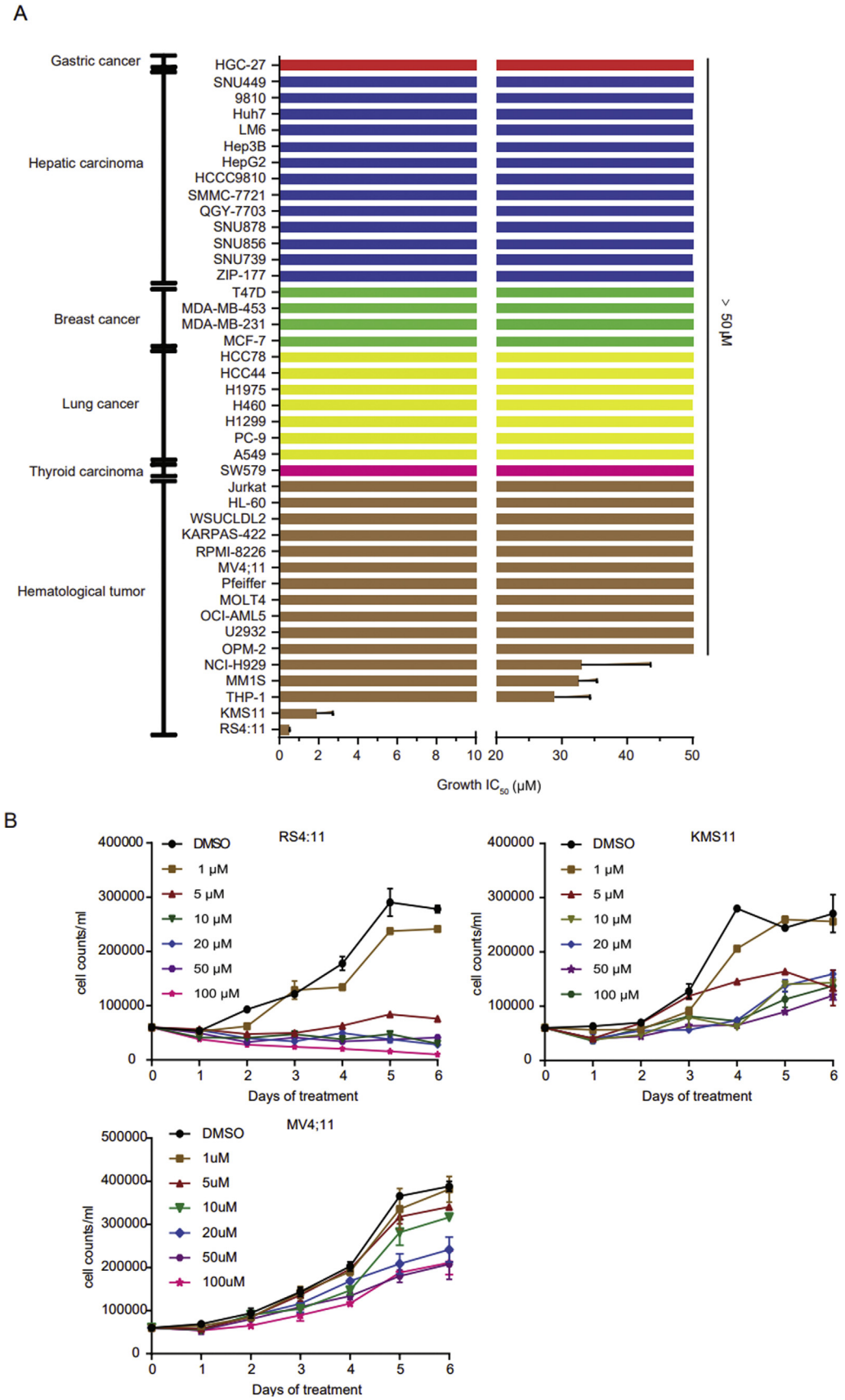

Fig. 5. Compound **9c** inhibits the proliferation of the human B cell precursor leukemia cell line RS4:11 and the human myeloma cell line KMS11 *in vitro*. (A) The effects of compound **9c** on the growth of 42 cell lines. The cell lines were treated with varying concentrations of compound **9c** for 6 days before cell growth was evaluated. The x-axis represents the growth IC_{50} value. (B) Dose-dependent and time-dependent effects of compound **9c** on cell proliferation in RS4:11 and KMS11 cells. Growth is expressed as cell counts. RS4:11 and

135.16, 131.45, 130.54, 128.36, 127.22, 126.82, 126.44, 126.06, 125.84, 125.46, 123.81, 123.37, 118.60, 42.57. ESI-LRMS *m/z*: 277.0 $[M + H]^+$. ESI-HRMS calcd for $C_{18}H_{17}N_2O$ $[M + H]^+$ 277.1335, found 277.1336.

*4.1.2. N-benzyl-1H-indole-4-carboxamide (**9a**)*

Compound **9a** was prepared in a similar manner as described for compound **8**. Yield: 89%. Mp 111–112 °C. ^{1}H NMR (400 MHz, DMSO-d_6) δ 11.29 (s, 1H), 8.79 (t, J = 6.1 Hz, 1H), 7.55 (dt, J = 8.1, 1.0 Hz, 1H), 7.48 (dd, J = 7.3, 0.9 Hz, 1H), 7.43 (t, J = 2.8 Hz, 1H), 7.39–7.31 (m, 4H), 7.24 (ddt, J = 8.6, 6.3, 1.8 Hz, 1H), 7.14 (dd, J = 8.1, 7.4 Hz, 1H), 6.86 (ddd, J = 3.0, 2.0, 0.9 Hz, 1H), 4.52 (d, J = 6.1 Hz, 2H). ^{13}C NMR (125 MHz, DMSO-d_6) δ 167.77, 140.12, 136.54, 128.20, 127.13, 126.56, 126.41, 125.93, 120.10, 118.42, 114.14, 101.80, 42.42. ESI-LRMS *m/z*: 250.9 $[M + H]^+$. ESI-HRMS calcd for $C_{16}H_{15}N_2O$ $[M + H]^+$ 251.1179, found 251.1175.

*4.1.3. N-benzylquinoline-5-carboxamide (**9b**)*

Compound **9b** was prepared in a similar manner as described for compound **8**. Yield: 83%. Mp 149–151 °C. ^{1}H NMR (400 MHz, DMSO-d_6) δ 9.22 (t, J = 6.1 Hz, 1H), 8.95 (dd, J = 4.1, 1.7 Hz, 1H), 8.66 (ddd, J = 8.6, 1.7, 0.9 Hz, 1H), 8.16–8.11 (m, 1H), 7.84–7.79 (m, 2H), 7.59 (dd, J = 8.6, 4.1 Hz, 1H), 7.43–7.35 (m, 4H), 7.28 (ddt, J = 8.6, 6.2, 1.7 Hz, 1H), 4.56 (d, J = 6.0 Hz, 2H). ^{13}C NMR (125 MHz, DMSO-d_6) δ 167.46, 150.77, 147.60, 139.37, 134.47, 133.68, 131.09, 128.51, 128.36, 127.21, 126.82, 125.81, 125.18, 121.98, 42.61. ESI-LRMS *m/z*: 263.0 $[M + H]^+$. ESI-HRMS calcd for $C_{17}H_{15}N_2O$ $[M + H]^+$ 263.1179, found 263.1174.

*4.1.4. 5-Acetamidonaphthalene-1-sulfonic acid (**14**)*

5-Aminonaphthalene-1-sulfonic acid **13** (15.0 g, 67.19 mmol) was dissolved in anhydrous DCM (50 mL), and triethylamine (10.27 mL, 73.91 mmol) was added followed by the dropwise addition of acetylchloride (5.27 mL, 73.91 mmol) at 0 °C. After stirring 8 h at room temperature, TLC showed completion of the reaction and solid was precipitated. The resulting mixture was filtered, and the filter cake was dried to afford compound **14** (16.3 g) as a purple solid, which was used without further purification. ESI-LRMS *m/z*: 264.0 $[M - H]^-$

*4.1.5. 5-Acetamidonaphthalene-1-sulfonyl chloride (**15**)*

Compound **14** (16.3 g, 61.44 mmol) and PCl_5 (19.19 g, 92.17 mmol) were dissolved in anhydrous DCM (100 mL), and the reaction mixture was heated at 40 °C. After 4 h, the reaction mixture was cooled down, and petroleum ether (100 mL) was added and triturated under ultrasound. Then the mixture was filtered, and the resulting filtrate was neutralized by saturated $NaHCO_3$ in an ice bath. A large amount of solid was subsequently precipitated and these solids was filtered, washed with methanol and dried to afford compound **15** as an earthy yellow solid (13.7 g, yield: 78%). ^{1}H NMR (400 MHz, DMSO-d_6) δ 9.94 (s, 1H), 8.70 (d, J = 8.6 Hz, 1H), 8.04 (dd, J = 8.5, 1.1 Hz, 1H), 7.97 (dd, J = 7.1, 1.2 Hz, 1H), 7.59 (d, J = 7.2 Hz, 1H), 7.51–7.41 (m, 2H), 2.17 (s, 3H). ESI-LRMS *m/z*: 282.0 $[M - H]^-$.

*4.1.6. N-(5-(N-benzylsulfamoyl)naphthalen-1-yl)acetamide (**11t**)*

To a stirred mixture of compound **15** (13.7 g, 48.29 mmol) and trimethylamine (8.05 mL, 57.94 mmol) in acetonitrile (100 mL) were added benzylamine (6.34 mL, 57.94 mmol) dropwise at room temperature. After 5 h, TLC showed completion of the reaction, and the reaction mixture was concentrated under vacuum. Then the resulting mixture was diluted with water (50 mL) and extracted with DCM (40 mL x 3). The combined organic layer was washed with brine (40 mL x 2), dried over anhydrous Na_2SO_4, then concentrated under vacuum and purified by silica gel column chromatography (DCM/MeOH = 50/1–20/1) to afford compound **11t** as a white solid (14.9 g, yield: 87%). Mp 193–194 °C. ^{1}H NMR (400 MHz, DMSO-d_6) δ 10.08 (s, 1H), 8.57–8.51 (m, 2H), 8.33 (d, J = 8.5 Hz, 1H), 8.14 (dd, J = 7.3, 1.1 Hz, 1H), 7.76 (d, J = 7.4 Hz, 1H), 7.71–7.61 (m, 2H), 7.25–7.10 (m, 5H), 4.03 (d, J = 6.2 Hz, 2H), 2.20 (s, 3H). ^{13}C NMR (125 MHz, DMSO-d_6) δ 169.09, 137.69, 136.14, 134.58, 128.86, 128.47, 128.26, 128.06, 127.42, 127.05, 124.17, 122.93, 122.07, 45.94, 23.43. ESI-LRMS *m/z*: 355.1 $[M + H]^+$. ESI-HRMS calcd for $C_{19}H_{19}N_2O_3S$ $[M + H]^+$ 355.1111, found 355.1116.

*4.1.7. 5-Amino-N-benzylnaphthalene-1-sulfonamide hydrochloride (**9c**)*

Compound **11t** (150 mg, 0.423 mmol) was dissolved in ethanol (3 mL) and 6 *N* HCl (3 mL), and the mixture was refluxed for 12 h. After cooling to room temperature, a large amount of solid was precipitated, and then filtered and dried to afford compound **9c** as a white solid (131 mg, yield: 88%).

Mp 176–178 °C. ^{1}H NMR (400 MHz, DMSO-d_6) δ 8.61 (t, J = 6.2 Hz, 1H), 8.49 (d, J = 8.6 Hz, 1H), 8.35 (d, J = 8.6 Hz, 1H), 8.18 (d, J = 7.3 Hz, 1H), 7.68 (dt, J = 11.6, 8.1 Hz, 2H), 7.59 (d, J = 7.3 Hz, 1H), 7.22–7.12 (m, 5H), 4.03 (d, J = 6.1 Hz, 2H). ^{13}C NMR (125 MHz, DMSO-d_6) δ 137.64, 136.31, 133.51, 128.95, 128.48, 128.06, 127.78, 127.65, 127.43, 127.08, 126.46, 124.56, 121.74, 118.27, 45.95. ESI-LRMS *m/z*: 313.0 $[M + H]^+$. ESI-HRMS calcd for $C_{17}H_{17}N_2O_2S$ $[M + H]^+$ 313.1005, found 313.1014.

*4.1.8. 6-Amino-N-benzylnaphthalene-1-sulfonamide hydrochloride (**10a**)*

Compound **10a** was prepared in a similar manner as described for compound **9c**. Yield: 82%. Mp 215–217 °C. ^{1}H NMR (400 MHz, DMSO-d_6) δ 8.88 (s, 2H), 8.67 (d, J = 9.2 Hz, 1H), 8.56 (t, J = 6.2 Hz, 1H), 8.15 (dt, J = 8.5, 1.0 Hz, 1H), 8.03 (dd, J = 7.3, 1.2 Hz, 1H), 7.79 (d, J = 2.2 Hz, 1H), 7.60 (dd, J = 8.3, 7.3 Hz, 1H), 7.54 (dd, J = 9.2, 2.3 Hz, 1H), 7.21–7.10 (m, 5H), 4.02 (d, J = 6.2 Hz, 2H). ^{13}C NMR (125 MHz, DMSO-d_6) δ 138.08, 136.49, 135.07, 133.11, 128.49, 127.89, 127.56, 127.49, 126.86, 125.84, 124.88, 122.51, 117.74, 46.41. ESI-LRMS *m/z*: 311.1 $[M - H]^-$. ESI-HRMS calcd for $C_{17}H_{15}N_2O_2S$ $[M - H]^-$ 311.0860, found 311.0860.

*4.1.9. 5-Amino-N-benzylnaphthalene-2-sulfonamide hydrochloride (**10b**)*

Compound **10b** was prepared in a similar manner as described for compound **9c**. Yield: 80%. Mp 235–237 °C. ^{1}H NMR (400 MHz, DMSO-d_6) δ 8.86 (s, 2H), 8.44 (d, J = 1.9 Hz, 1H), 8.35 (t, J = 6.3 Hz, 1H), 8.27 (dt, J = 9.0, 0.8 Hz, 1H), 7.93 (d, J = 7.2 Hz, 1H), 7.91 (dd, J = 9.0, 2.0 Hz, 1H), 7.62 (t, J = 7.7 Hz, 1H), 7.57 (dd, J = 7.5, 1.4 Hz, 1H), 7.28–7.22 (m, 4H), 7.22–7.16 (m, 1H), 4.03 (d, J = 6.1 Hz, 2H). ^{13}C NMR (125 MHz, DMSO-d_6) δ 138.28, 137.58, 134.09, 132.76, 128.18, 127.63, 127.54, 127.12, 126.27, 125.14, 123.95, 121.98, 118.69, 109.51, 46.13. ESI-LRMS *m/z*: 311.1 $[M - H]^-$. ESI-HRMS calcd for $C3_7H_{15}N_2O_2S$ $[M - H]^-$ 311.0860, found 311.0863.

*4.1.10. 6-Amino-N-benzylnaphthalene-2-sulfonamide hydrochloride (**10c**)*

Compound **10c** was prepared in a similar manner as described for compound **9c**. Yield: 82%. Mp 239–241 °C. ^{1}H NMR (400 MHz, DMSO-d_6) δ 9.19 (s, 2H), 8.36 (d, J = 1.8 Hz, 1H), 8.24 (t, J = 6.4 Hz, 1H), 8.11 (d, J = 8.8 Hz, 1H), 8.01 (d, J = 8.7 Hz, 1H), 7.79 (dd, J = 8.7,

KMS11 cells were treated with compound **9c** (0, 1, 5, 10, 20, 50, and 100 μM) for 6 days, and the number of cells in each treatment group was determined daily. Growth is expressed as cell counts. Data are reported as the mean ± SD.

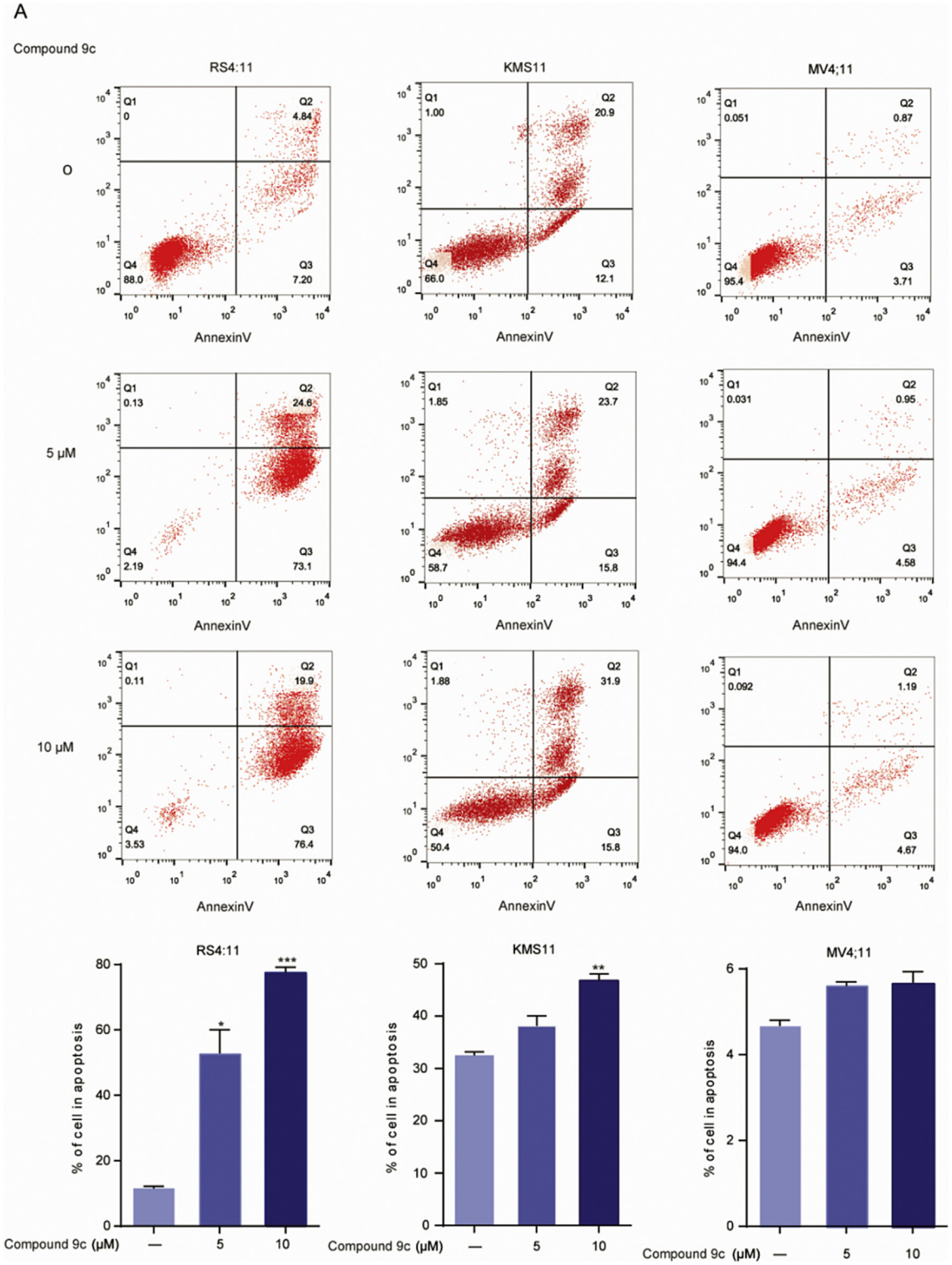

Fig. 6. In RS4:11 and KMS11 cells, compound **9c** induces cell apoptosis and arrests the cell cycle at the G0/G1 phase. (A) RS4:11, KMS11, and MV4;11 cells were treated with compound **9c** (at 5 and 10 μM) for 72 h, and the effects on apoptosis were examined by flow cytometry. (B) RS4:11, KMS11, and MV4;11 cells were incubated with compound **9c** (at 5 and 10 μM) for 72 h, and the proportions of cells in each cell cycle phase were determined by flow cytometry.

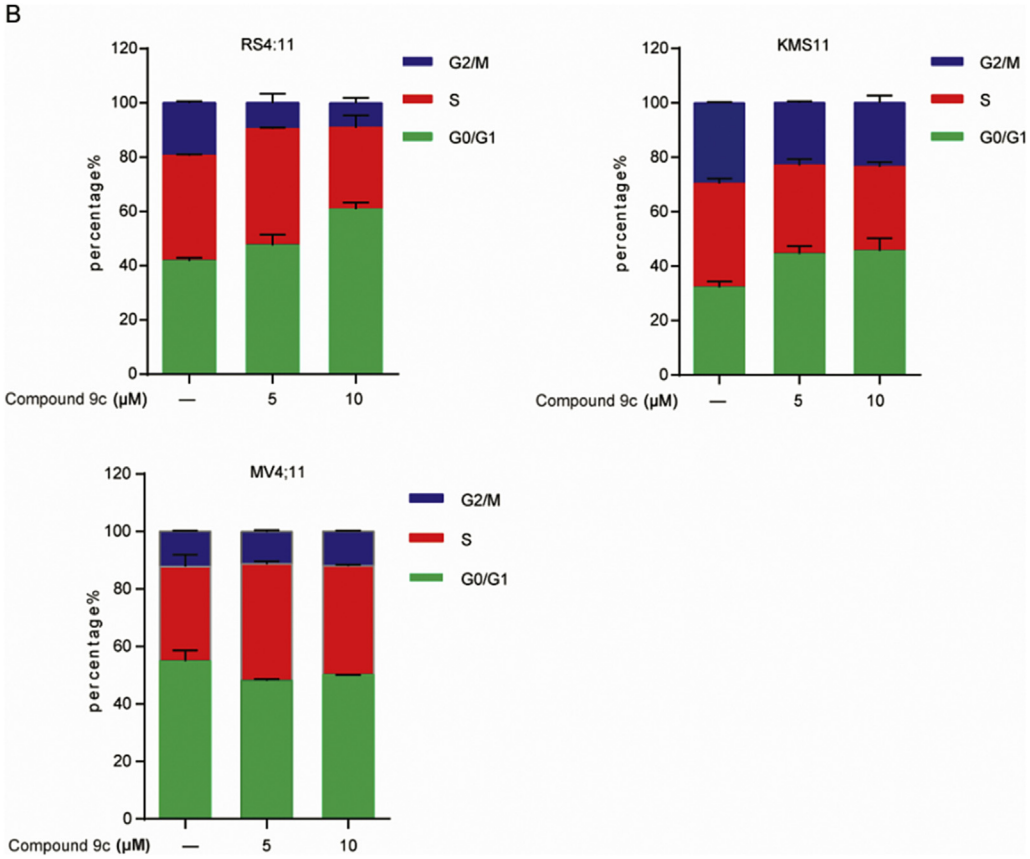

Fig. 6. (*continued*).

1.9 Hz, 1H), 7.65 (d, J = 2.0 Hz, 1H), 7.45 (dd, J = 8.7, 2.1 Hz, 1H), 7.26–7.20 (m, 4H), 7.20–7.14 (m, 1H), 4.00 (d, J = 5.8 Hz, 2H). ^{13}C NMR (125 MHz, DMSO-d_6) δ 139.15, 137.65, 135.77, 135.03, 130.77, 128.14, 128.07, 127.90, 127.55, 127.37, 127.05, 123.08, 121.59, 114.79, 46.12. ESI-LRMS *m/z*: 311.0 [M − H]$^-$. ESI-HRMS calcd for $C_{17}H_{15}N_2O_2S$ [M − H]$^-$ 311.0860, found 311.0866.

4.1.11. 4-Amino-N-benzylnaphthalene-1-sulfonamide hydrochloride (**10d**)

Compound **10d** was prepared in a similar manner as described for compound **9c**. Yield: 85%. Mp 166–168 °C. ^{1}H NMR (400 MHz, CD_3OD) δ 8.83–8.77 (m, 1H), 8.17 (d, J = 7.9 Hz, 1H), 8.10–8.04 (m, 1H), 7.85–7.77 (m, 2H), 7.49 (d, J = 7.9 Hz, 1H), 7.09–6.95 (m, 5H), 4.09 (s, 2H). ^{13}C NMR (125 MHz, DMSO-d_6) δ 148.12, 138.09, 131.34, 129.45, 128.00, 127.60, 127.44, 126.90, 124.96, 124.70, 123.07, 122.79, 121.77, 106.15, 45.79. ESI-LRMS *m/z*: 311.1 [M − H]$^-$. ESI-HRMS calcd for $C_{17}H_{15}N_2O_2S$ [M − H]$^-$ 311.0860, found 311.0867.

4.1.12. 5-Amino-N-phenylnaphthalene-1-sulfonamide hydrochloride (**11a**)

Compound **11a** was prepared in a similar manner as described for compound **9c**. Yield: 77%. Mp 206–207 °C. ^{1}H NMR (400 MHz, DMSO-d_6) δ 10.74 (s, 1H), 8.45 (d, J = 8.6 Hz, 1H), 8.35 (d, J = 8.5 Hz, 1H), 8.24 (d, J = 7.2 Hz, 1H), 7.68–7.60 (m, 2H), 7.45 (d, J = 7.4 Hz, 1H), 7.13 (t, J = 7.7 Hz, 2H), 7.01 (d, J = 7.9 Hz, 2H), 6.91 (t, J = 7.3 Hz, 1H), 5.28 (s, 2H). ^{13}C NMR (150 MHz, CD_3OD) δ 138.42, 137.27, 132.51, 130.43, 130.06, 129.37, 128.86, 128.72, 127.73, 127.14, 127.08, 125.61, 122.85, 121.61. ESI-LRMS *m/z*: 299.2 [M + H]$^+$. ESI-HRMS calcd for $C_{16}H_{15}N_2O_2S$ [M + H]$^+$ 299.0849, found 299.0848.

4.1.13. 5-Amino-N-phenethylnaphthalene-1-sulfonamide hydrochloride (**11b**)

Compound **11b** was prepared in a similar manner as described for compound **9c**. Yield: 80%. Mp 181–182 °C. ^{1}H NMR (400 MHz, DMSO-d_6) δ 8.37 (dd, J = 8.5, 5.4 Hz, 2H), 8.17–8.10 (m, 2H), 7.73–7.65 (m, 1H), 7.64–7.59 (m, 1H), 7.50 (d, J = 7.3 Hz, 1H), 7.19–7.09 (m, 3H), 7.05–7.00 (m, 2H), 3.04–2.98 (m, 2H), 2.60 (t, J = 7.4 Hz, 2H). ^{13}C NMR (125 MHz, DMSO-d_6) δ 138.94, 136.50, 134.45, 129.33, 128.97, 128.64, 128.24, 128.13, 126.83, 126.61, 124.90, 121.77, 118.32, 44.43, 35.82. ESI-LRMS *m/z*: 327.2 [M + H]$^+$. ESI-HRMS calcd for $C_{18}H_{19}N_2O_2S$ [M + H]$^+$ 327.1162, found 327.1167.

4.1.14. 5-Amino-N-(4-fluorobenzyl)naphthalene-1-sulfonamide hydrochloride (**11c**)

Compound **11c** was prepared in a similar manner as described for compound **9c**. Yield: 78%. Mp 191–193 °C. ^{1}H NMR (400 MHz, DMSO-d_6) δ 8.60 (t, J = 6.2 Hz, 1H), 8.40 (d, J = 8.7 Hz, 1H), 8.35 (d, J = 8.6 Hz, 1H), 8.14 (dd, J = 7.4, 1.1 Hz, 1H), 7.67 (dd, J = 7.6, 6.4 Hz, 1H), 7.63 (dd, J = 7.5, 6.4 Hz, 1H), 7.50 (d, J = 7.5 Hz, 1H), 7.20–7.12 (m, 2H), 7.05–6.95 (m, 2H), 4.01 (d, J = 6.1 Hz, 2H). ^{13}C NMR (125 MHz, CD_3OD) δ 163.34 (d, J = 244.4 Hz), 138.86, 134.43 (d, J = 3.1 Hz), 131.29, 130.68 (d, J = 8.2 Hz), 130.38, 129.24, 128.89, 128.48, 127.39, 127.33, 127.10, 122.69, 115.75 (d, J = 21.7 Hz), 46.93. ESI-LRMS *m/z*: 331.2 [M + H]$^+$. ESI-HRMS calcd for $C_{17}H_{16}FN_2O_2S$ [M + H]$^+$ 331.0911, found 331.0915.

4.1.15. 5-Amino-N-(4-methoxybenzyl)naphthalene-1-sulfonamide hydrochloride (**11d**)

Compound **11d** was prepared in a similar manner as described for compound **9c**. Yield: 86%. Mp 172–174 °C. ^{1}H NMR (400 MHz, DMSO-d_6) δ 8.47 (t, J = 6.1 Hz, 1H), 8.39 (d, J = 8.7 Hz, 1H), 8.35 (dt,

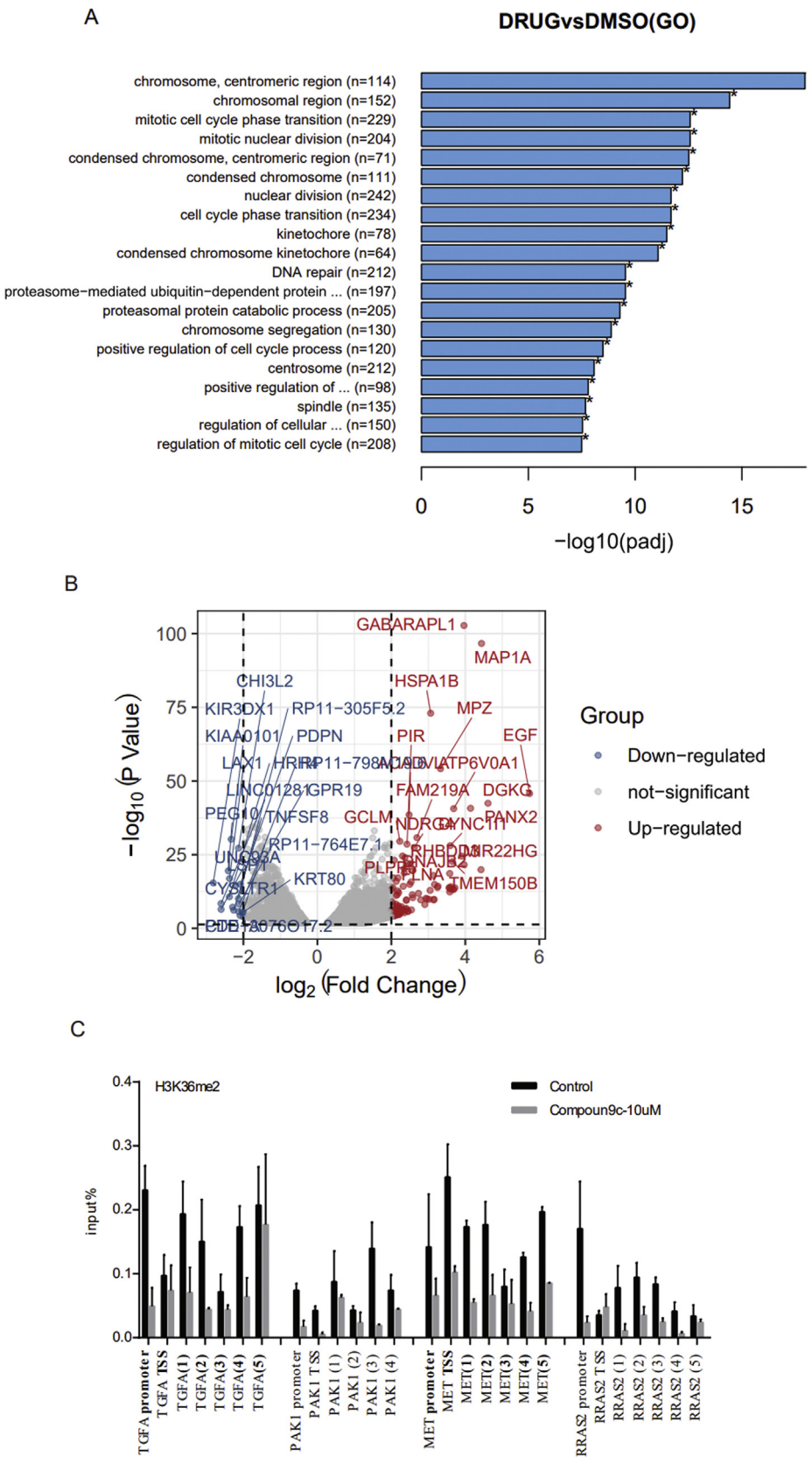

Fig. 7. Compound **9c** suppresses of the NSD2-target genes by decreased H3K36me2 level in the promoter regions. (A) GO analysis of the differential genes upon compound **9c** treatment identified by RNA-seq in RS4:11 cells. (B) Volcano plot showing the differentially expressed genes in RS4:11 cells treated with DMSO or compound **9c** (10 μM) for 72 h, the top 20 increased or decreased genes are labelled. (C) ChIP-qPCR analyses of H3K36me2 level in the promoter regions of the genes TGFA, MET, PAK1, and RRAS2.

Table 5
Pharmacokinetic profiles of compound **9c** in CD-1 mice[a].

Compd.	$T_{1/2}$ (h)	T_{max} (h)	C_{max} (ng/mL)	AUC (h*ng/mL)	CL (mL/min/kg)	MRT (h)	Vss (mL/kg)
9c (i.p.)	0.56 ± 0.06	0.083	433 ± 71.1	150 ± 33.9	–	0.531	–
9c (i.v.)	0.66 ± 0.03	–	–	204 ± 18.9	163 ± 16.1	0.396 ± 0.06	3854 ± 478

[a] Values are the average of three runs. $T_{1/2}$, half-life; T_{max}, time of maximum concentration; C_{max}, maximum concentration; AUC, area under the plasma concentration−time curve; CL, clearance; MRT, mean residence time; V_{ss}, volume of distribution; F, oral bioavailability. Dose: i.p. at 2.0 mg/kg. Dose: i.v. at 2.0 mg/kg (n = 3 per group).

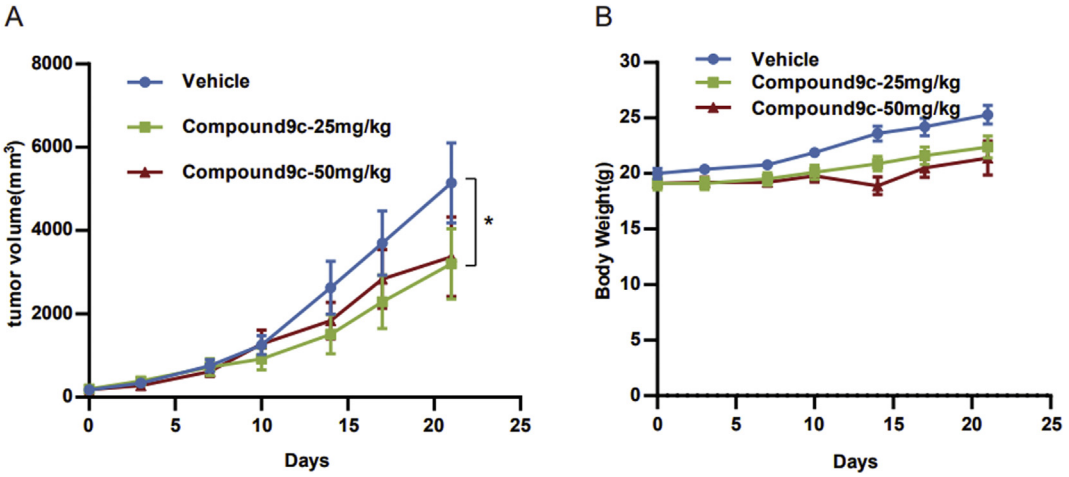

Fig. 8. Compound **9c** inhibits RS4:11 xenografts *in vivo*. (A) Tumor-bearing mice (n = 8 per group) were treated with compound **9c** (25 mg/kg and 50 mg/kg) daily for 21 days. The curve shows the tumor volume after 21 days of treatment with compound **9c** or vehicle. Data are shown as the mean ± SEM; *$P = 0.027$. (B) The corresponding curve of body weight after 21 days of treatment with compound **9c** or vehicle was shown. Error bars represent the mean ± SEM from eight individuals in each group.

J = 8.6, 1.1 Hz, 1H), 8.14 (dd, *J* = 7.3, 1.1 Hz, 1H), 7.66 (dd, *J* = 8.6, 7.4 Hz, 1H), 7.62 (dd, *J* = 8.7, 7.5 Hz, 1H), 7.47 (d, *J* = 7.5 Hz, 1H), 7.07−7.02 (m, 2H), 6.76−6.72 (m, 2H), 3.94 (d, *J* = 6.0 Hz, 2H), 3.68 (s, 3H). ^{13}C NMR (125 MHz, DMSO-d_6) δ 158.36, 136.32, 134.39, 129.50, 128.85, 128.82, 128.51, 127.82, 127.59, 126.20, 124.34, 120.99, 117.52, 113.48, 55.07, 45.47. ESI-LRMS *m/z*: 343.2 $[M + H]^+$. ESI-HRMS calcd for $C_{18}H_{19}N_2O_3S$ $[M + H]^+$ 343.1111, found 343.1119.

4.1.16. 5-Amino-N-(4-(trifluoromethyl)benzyl)naphthalene-1-sulfonamide hydrochloride (**11e**)

Compound **11e** was prepared in a similar manner as described for compound **9c**. Yield: 82%. Mp 178−180 °C. ^{1}H NMR (400 MHz, CD_3OD) δ 8.82 (dt, *J* = 8.4, 1.3 Hz, 1H), 8.32 (dd, *J* = 7.4, 1.0 Hz, 1H), 8.23 (d, *J* = 8.5 Hz, 1H), 7.81−7.70 (m, 3H), 7.39 (d, *J* = 8.1 Hz, 2H), 7.25 (d, *J* = 8.1 Hz, 2H), 4.20 (s, 2H). ^{13}C NMR (125 MHz, CD_3OD) δ 143.21, 138.66, 131.27, 130.43 (q, *J* = 32.2 Hz), 130.36, 129.58, 129.24, 128.87, 128.59, 127.30, 127.26, 127.14, 126.03 (q, *J* = 3.6 Hz), 125.54 (q, *J* = 271.1 Hz), 122.57, 47.06. ESI-LRMS *m/z*: 381.1 $[M + H]^+$. ESI-HRMS calcd for $C_{18}H_{16}F_3N_2O_2S$ $[M + H]^+$ 381.0879, found 381.0868.

4.1.17. 5-Amino-N-(4-cyanobenzyl)naphthalene-1-sulfonamide hydrochloride (**11f**)

Compound **11f** was prepared in a similar manner as described for compound **9c**. Yield: 77%. Mp 209−211 °C. ^{1}H NMR (500 MHz, CD_3OD) δ 8.83 (ddd, *J* = 8.1, 1.9, 1.0 Hz, 1H), 8.31 (dd, *J* = 7.4, 1.1 Hz, 1H), 8.22 (dt, *J* = 8.6, 1.1 Hz, 1H), 7.80−7.74 (m, 3H), 7.45−7.41 (m, 2H), 7.25−7.22 (m, 2H), 4.21 (s, 2H). ^{13}C NMR (125 MHz, CD_3OD) δ 144.42, 138.66, 133.01, 131.32, 130.31, 129.51, 129.24, 128.92, 128.61, 127.37, 127.34, 127.27, 122.83, 119.45, 112.03, 47.09. ESI-LRMS *m/z*: 336.0 $[M - H]^-$. ESI-HRMS calcd for $C_{18}H_{14}N_3O_2S$ $[M - H]^-$ 336.0812, found 336.0818.

4.1.18. 5-Amino-N-(3-cyanobenzyl)naphthalene-1-sulfonamide hydrochloride (**11g**)

Compound **11g** was prepared in a similar manner as described for compound **9c**. Yield: 80%. Mp 212−214 °C. ^{1}H NMR (500 MHz, DMSO-d_6) δ 8.71 (t, *J* = 6.3 Hz, 1H), 8.37 (d, *J* = 8.7 Hz, 1H), 8.32 (d, *J* = 8.5 Hz, 1H), 8.14 (dd, *J* = 7.3, 1.0 Hz, 1H), 7.64 (ddd, *J* = 8.7, 7.5, 3.5 Hz, 2H), 7.55 (dt, *J* = 7.6, 1.4 Hz, 1H), 7.52 (s, 1H), 7.49 (d, *J* = 7.4 Hz, 1H), 7.41 (dt, *J* = 7.8, 1.4 Hz, 1H), 7.30 (t, *J* = 7.7 Hz, 1H), 4.10 (d, *J* = 6.2 Hz, 2H). ^{13}C NMR (125 MHz, DMSO-d_6) δ 139.23, 135.83, 134.69, 132.11, 130.79, 130.69, 129.14, 129.03, 128.34, 127.92, 127.81, 126.00, 124.16, 120.42, 118.52, 117.21, 110.78, 45.01. ESI-LRMS *m/z*: 336.0 $[M - H]^-$. ESI-HRMS calcd for $C_{18}H_{14}N_3O_2S$ $[M - H]^-$ 336.0812, found 336.0812.

4.1.19. 4-(((5-Aminonaphthalene)-1-sulfonamido)methyl)benzoic acid hydrochloride (**11h**)

Compound **11h** was prepared in a similar manner as described for compound **9c**. Yield: 72%. Mp 259−260 °C. ^{1}H NMR (400 MHz, DMSO-d_6) δ 8.72 (t, *J* = 6.2 Hz, 1H), 8.47 (d, *J* = 8.6 Hz, 1H), 8.37 (d, *J* = 8.6 Hz, 1H), 8.18 (dd, *J* = 7.4, 1.0 Hz, 1H), 7.79 (d, *J* = 8.3 Hz, 2H), 7.73−7.69 (m, 1H), 7.68−7.65 (m, 1H), 7.58 (d, *J* = 7.5 Hz, 1H), 7.31 (d, *J* = 8.4 Hz, 2H), 4.10 (d, *J* = 6.2 Hz, 2H). ^{13}C NMR (125 MHz, DMSO-d_6) δ 167.02, 143.02, 136.02, 134.73, 129.54, 129.14, 128.88, 128.47, 127.94, 127.81, 127.41, 126.16, 124.24, 120.62, 117.34, 45.57. ESI-LRMS *m/z*: 355.0 $[M - H]^-$. ESI-HRMS calcd for $C_{18}H_{15}N_2O_4S$ $[M - H]^-$ 355.0758, found 355.0759.

4.1.20. 5-Amino-N-(pyridin-4-ylmethyl)naphthalene-1-sulfonamide dihydrochloride (**11i**)

Compound **11i** was prepared in a similar manner as described for compound **9c**. Yield: 83%. Mp 173−175 °C. ^{1}H NMR (400 MHz, DMSO-d_6) δ 9.12 (t, *J* = 6.3 Hz, 1H), 8.75 (d, *J* = 6.6 Hz, 2H), 8.39 (d,

J = 8.6 Hz, 1H), 8.34 (d, J = 8.7 Hz, 1H), 8.16 (dd, J = 7.4, 1.0 Hz, 1H), 7.86 (d, J = 6.5 Hz, 2H), 7.66 (ddd, J = 8.6, 7.4, 4.3 Hz, 2H), 7.49 (d, J = 7.5 Hz, 1H), 4.36 (d, J = 6.3 Hz, 2H). ^{13}C NMR (150 MHz, CD_3OD) δ 161.93, 142.34, 137.65, 131.44, 130.24, 130.20, 129.06, 128.94, 127.99, 127.25, 126.76, 126.60, 122.63, 46.44. ESI-LRMS *m/z*: 312.0 [M − H]$^-$. ESI-HRMS calcd for $C_{16}H_{14}N_3O_2S$ [M − H]$^-$ 312.0812, found 312.0810.

4.1.21. 5-Amino-N-(thiophen-3-ylmethyl)naphthalene-1-sulfonamide hydrochloride (**11j**)

Compound **11j** was prepared in a similar manner as described for compound **9c**. Yield: 78%. Mp 146−148 °C. ^{1}H NMR (500 MHz, CD_3OD) δ 8.85−8.81 (m, 1H), 8.31 (dd, J = 7.4, 1.1 Hz, 1H), 8.21 (dt, J = 8.6, 1.1 Hz, 1H), 7.79−7.73 (m, 3H), 7.04 (dd, J = 5.0, 3.0 Hz, 1H), 6.93−6.91 (m, 1H), 6.64 (dd, J = 5.0, 1.3 Hz, 1H), 4.14 (s, 2H). ^{13}C NMR (125 MHz, CD_3OD) δ 139.06, 138.82, 131.25, 130.42, 129.01, 128.93, 128.39, 128.02, 127.55, 127.39, 127.07, 126.65, 123.49, 122.79, 42.74. ESI-LRMS *m/z*: 317.0 [M − H]$^-$. ESI-HRMS calcd for $C_{15}H_{13}N_2O_2S_2$ [M − H]$^-$ 317.0424, found 317.0428.

4.1.22. 5-Amino-N-(cyclohexylmethyl)naphthalene-1-sulfonamide hydrochloride (**11k**)

Compound **11k** was prepared in a similar manner as described for compound **9c**. Yield: 87%. Mp 218−220 °C. ^{1}H NMR (500 MHz, DMSO-d_6) δ 8.41 (d, J = 8.7 Hz, 1H), 8.36 (d, J = 8.5 Hz, 1H), 8.14 (d, J = 7.2 Hz, 1H), 7.95 (t, J = 5.9 Hz, 1H), 7.69 (dd, J = 8.5, 7.3 Hz, 1H), 7.63 (dd, J = 8.7, 7.5 Hz, 1H), 7.49 (d, J = 7.5 Hz, 1H), 2.60 (t, J = 6.4 Hz, 2H), 1.59−1.47 (m, 5H), 1.25 (ttt, J = 10.2, 6.7, 3.0 Hz, 1H), 1.07−0.96 (m, 3H), 0.76−0.65 (m, 2H). ^{13}C NMR (125 MHz, DMSO-d_6) δ 136.27, 134.76, 128.70, 128.54, 127.77, 127.51, 126.08, 124.24, 120.63, 117.11, 48.64, 37.23, 30.02, 25.85, 25.16. ESI-LRMS *m/z*: 317.1 [M − H]$^-$. ESI-HRMS calcd for $C_{17}H_{21}N_2O_2S$ [M − H]$^-$ 317.1329, found 317.1331.

4.1.23. 5-Amino-N-(piperidin-3-ylmethyl)naphthalene-1-sulfonamide dihydrochloride (**11l**)

Compound **11l** was prepared in a similar manner as described for compound **9c**. Yield: 75%. Mp 272−274 °C. ^{1}H NMR (500 MHz, DMSO-d_6) δ 9.17 (d, J = 11.2 Hz, 1H), 8.96 (q, J = 10.8 Hz, 1H), 8.44 (d, J = 8.8 Hz, 1H), 8.41 (d, J = 8.6 Hz, 1H), 8.24 (t, J = 6.2 Hz, 1H), 8.15 (d, J = 7.2 Hz, 1H), 7.72 (dd, J = 8.5, 7.4 Hz, 1H), 7.67 (t, J = 8.0 Hz, 1H), 7.59 (d, J = 7.5 Hz, 1H), 3.19−3.08 (m, 2H), 2.76−2.68 (m, 2H), 2.67−2.59 (m, 1H), 2.49−2.42 (m, 1H), 1.93−1.83 (m, 1H), 1.72−1.61 (m, 2H), 1.61−1.50 (m, 1H), 1.12−1.00 (m, 1H). ^{13}C NMR (125 MHz, DMSO-d_6) δ 135.80, 133.96, 128.84, 128.43, 127.88, 126.42, 124.42, 121.17, 117.98, 45.75, 45.20, 43.10, 33.58, 25.59, 21.11. ESI-LRMS *m/z*: 318.0 [M − H]$^-$. ESI-HRMS calcd for $C_{16}H_{20}N_3O_2S$ [M − H]$^-$ 318.1282, found 318.1281.

4.1.24. 5-Amino-N-((1-methylpiperidin-4-yl)methyl)naphthalene-1-sulfonamide dihydrochloride (**11m**)

Compound **11m** was prepared in a similar manner as described for compound **9c**. Yield: 80%. Mp 231−232 °C. ^{1}H NMR (500 MHz, CD_3OD) δ 8.87−8.84 (m, 1H), 8.36 (dd, J = 7.4, 1.1 Hz, 1H), 8.30 (dt, J = 8.6, 1.1 Hz, 1H), 7.86 (dd, J = 8.6, 7.4 Hz, 1H), 7.82−7.78 (m, 1H), 7.77 (dd, J = 7.5, 1.6 Hz, 1H), 3.46 (dp, J = 12.5, 1.9 Hz, 2H), 2.92 (td, J = 13.0, 2.9 Hz, 2H), 2.85−2.79 (m, 5H), 1.92 (ddd, J = 13.3, 4.3, 2.4 Hz, 2H), 1.78−1.68 (m, 1H), 1.46−1.36 (m, 2H). ^{13}C NMR (125 MHz, CD_3OD) δ 138.33, 131.04, 130.39, 129.45, 129.06, 128.66, 127.47, 127.39, 127.25, 122.86, 55.28, 48.39, 43.84, 35.03, 28.42. ESI-LRMS *m/z*: 332.1 [M − H]$^-$. ESI-HRMS calcd for $C_{17}H_{22}N_3O_2S$ [M − H]$^-$ 332.1438, found 332.1442.

4.1.25. 5-Amino-N-(trans-2-phenylcyclopropyl)naphthalene-1-sulfonamide hydrochloride (**11n**)

Compound **11n** was prepared in a similar manner as described for compound **9c**. Yield: 82%. Mp 187−189 °C. ^{1}H NMR (500 MHz, DMSO-d_6) δ 8.62 (d, J = 2.7 Hz, 1H), 8.42 (t, J = 8.2 Hz, 2H), 8.17 (dd, J = 7.3, 1.0 Hz, 1H), 7.68 (dd, J = 8.6, 7.4 Hz, 1H), 7.63−7.56 (m, 2H), 7.18−7.13 (m, 2H), 7.11−7.06 (m, 1H), 6.76−6.70 (m, 2H), 2.26 (ddt, J = 7.3, 4.5, 2.8 Hz, 1H), 1.63 (ddd, J = 9.6, 6.6, 3.1 Hz, 1H), 1.06−1.00 (m, 2H). ^{13}C NMR (125 MHz, DMSO-d_6) δ 140.04, 135.71, 133.95, 129.92, 128.55, 128.12, 128.03, 127.89, 126.34, 125.75, 125.62, 124.52, 121.19, 117.96, 33.88, 23.48, 14.26. ESI-LRMS *m/z*: 337.0 [M − H]$^-$. ESI-HRMS calcd for $C_{19}H_{17}N_2O_2S$ [M − H]$^-$ 337.1016, found 337.1021.

4.1.26. 5-Amino-N-(tert-butyl)naphthalene-1-sulfonamide hydrochloride (**11o**)

Compound **11o** was prepared in a similar manner as described for compound **9c**. Yield: 85%. Mp 184−185 °C. ^{1}H NMR (500 MHz, DMSO-d_6) δ 8.57 (d, J = 7.8 Hz, 1H), 8.36 (d, J = 8.5 Hz, 1H), 8.26 (d, J = 7.3 Hz, 1H), 7.86 (s, 1H), 7.77−7.72 (m, 1H), 7.71−7.64 (m, 2H), 1.05 (s, 9H). ^{13}C NMR (125 MHz, DMSO-d_6) δ 139.45, 132.16, 128.78, 128.53, 127.43, 127.40, 126.74, 124.96, 122.90, 119.16, 53.55, 29.66. ESI-LRMS *m/z*: 277.2 [M − H]$^-$. ESI-HRMS calcd for $C_{14}H_{17}N_2O_2S$ [M − H]$^-$ 277.1016, found 277.1012.

4.1.27. 5-Amino-N-benzyl-N-methylnaphthalene-1-sulfonamide hydrochloride (**11p**)

Compound **11p** was prepared in a similar manner as described for compound **9c**. Yield: 78%. Mp 174−175 °C. ^{1}H NMR (400 MHz, DMSO-d_6) δ 8.44 (d, J = 8.6 Hz, 1H), 8.39 (d, J = 8.9 Hz, 1H), 8.21 (d, J = 7.3 Hz, 1H), 7.74 (t, J = 8.0 Hz, 1H), 7.68 (t, J = 8.1 Hz, 1H), 7.51 (d, J = 7.1 Hz, 1H), 7.37−7.26 (m, 5H), 4.39 (s, 2H), 2.68 (s, 3H). ^{13}C NMR (125 MHz, CD_3OD) δ 137.15, 137.12, 131.57, 130.96, 129.67, 129.51, 129.42, 129.22, 128.99, 128.69, 127.69, 127.55, 127.46, 122.90, 54.57, 34.36. ESI-LRMS *m/z*: 327.3 [M + H]$^+$. ESI-HRMS calcd for $C_{18}H_{19}N_2O_2S$ [M + H]$^+$ 327.1162, found 327.1156.

4.1.28. 5-((4-Benzylpiperidin-1-yl)sulfonyl)naphthalen-1-amine hydrochloride (**11q**)

Compound **11q** was prepared in a similar manner as described for compound **9c**. Yield: 75%. Mp 181−183 °C. ^{1}H NMR (500 MHz, DMSO-d_6) δ 8.42 (d, J = 8.5 Hz, 1H), 8.35 (d, J = 8.8 Hz, 1H), 8.15 (dd, J = 7.4, 1.1 Hz, 1H), 7.72 (dd, J = 8.5, 7.3 Hz, 1H), 7.63 (dd, J = 8.8, 7.5 Hz, 1H), 7.48 (d, J = 7.4 Hz, 1H), 7.23 (t, J = 7.5 Hz, 2H), 7.16−7.12 (m, 1H), 7.11−7.07 (m, 2H), 3.70 (dt, J = 12.9, 2.8 Hz, 2H), 2.55−2.47 (m, 2H), 2.43 (d, J = 6.7 Hz, 2H), 1.61−1.50 (m, 3H), 1.15−1.04 (m, 2H). ^{13}C NMR (125 MHz, DMSO-d_6) δ 139.73, 135.13, 133.38, 130.24, 129.10, 128.93, 128.33, 128.15, 128.12, 126.18, 125.82, 124.26, 120.30, 117.04, 45.42, 41.72, 36.26, 31.09. ESI-LRMS *m/z*: 381.0 [M + H]$^+$. ESI-HRMS calcd for $C_{22}H_{25}N_2O_2S$ [M + H]$^+$ 381.1631, found 381.1631.

4.1.29. N-benzylnaphthalene-1-sulfonamide (**11r**)

Compound **11r** was prepared in a similar manner as described for compound **9c**. Yield: 89%. Mp 131−133 °C. ^{1}H NMR (500 MHz, DMSO-d_6) δ 8.68 (dd, J = 8.5, 1.1 Hz, 1H), 8.51 (t, J = 6.2 Hz, 1H), 8.19 (d, J = 8.2 Hz, 1H), 8.12 (dd, J = 7.3, 1.3 Hz, 1H), 8.07 (dd, J = 8.1, 1.4 Hz, 1H), 7.71 (ddd, J = 8.5, 6.9, 1.6 Hz, 1H), 7.66 (ddd, J = 8.0, 6.8, 1.3 Hz, 1H), 7.61 (dd, J = 8.2, 7.3 Hz, 1H), 7.20−7.11 (m, 5H), 4.03 (d, J = 6.1 Hz, 2H). ^{13}C NMR (125 MHz, DMSO-d_6) δ 137.64, 135.82, 133.81, 133.60, 128.85, 128.35, 127.97, 127.73, 127.50, 127.37, 126.97, 126.76, 124.73, 124.43, 45.91. ESI-LRMS *m/z*: 296.0 [M − H]$^-$. ESI-HRMS calcd for $C_{17}H_{14}NO_2S$ [M − H]$^-$ 296.0751, found 296.0753.

4.1.30. N-benzyl-5-(dimethylamino)naphthalene-1-sulfonamide hydrochloride (**11s**)

Compound **11s** was prepared in a similar manner as described for compound **9c**. Yield: 88%. Mp 176−177 °C. ^{1}H NMR (500 MHz, DMSO-d_6) δ 8.77 (d, J = 8.9 Hz, 1H), 8.65 (t, J = 6.3 Hz, 1H), 8.60 (d,

J = 8.4 Hz, 1H), 8.18 (d, J = 7.3 Hz, 1H), 7.80–7.62 (m, 3H), 7.16–7.07 (m, 5H), 4.04 (d, J = 6.1 Hz, 2H), 3.10 (s, 6H). ^{13}C NMR (125 MHz, DMSO-d_6) δ 137.48, 136.74, 128.81, 128.24, 127.93, 127.56, 127.42, 127.21, 126.98, 124.97, 123.33, 117.88, 45.97, 45.87. ESI-LRMS *m/z*: 341.2 [M + H]$^+$. ESI-HRMS calcd for $C_{19}H_{21}N_2O_2S$ [M + H]$^+$ 341.1318, found 341.1319.*N-Benzyl-5-((cyclopropylmethyl)amino) naphthalene-1-sulfonamide hydrochloride (**11u**).*

To a stirred solution of compound **9c** (150 mg, 0.430 mmol) in anhydrous MeOH (8 mL) was added trimethylamine (60 μL, 0.430 mmol) at room temperature. After 10 min, cyclopropanecarboxaldehyde **19a** (32 μL, 0.430 mmol) and acetic acid (25 μL, 0.430 mmol) were added to the reaction mixture. Then, sodium cyanoborohydride (30 mg, 0.473 mmol) was added after 0.5 h. After 5 h, TLC showed completion of the reaction. The reaction mixture was concentrated and diluted with water (10 mL), then extracted with DCM (5 mL x 3). The combined layer was concentrated under vacuum and purified by silica gel column chromatography (DCM/MeOH = 50/1–20/1) to afford white solid, which was subsequently dissolved in 4 *N* HCl in dioxane (5 mL) and stirred for 2 h at room temperature. Finally, the reaction mixture was concentrated to afford compound **11u** as a white solid (117 mg, yield: 68%). Mp 160–161 °C. ^{1}H NMR (500 MHz, DMSO-d_6) δ 8.52 (dt, J = 8.5, 1.1 Hz, 1H), 8.47 (t, J = 6.2 Hz, 1H), 8.21–8.15 (m, 1H), 8.12 (dd, J = 7.4, 1.1 Hz, 1H), 7.60–7.54 (m, 3H), 7.21–7.10 (m, 5H), 4.00 (d, J = 6.1 Hz, 2H), 3.19 (d, J = 6.9 Hz, 2H), 1.21–1.14 (m, 1H), 0.54–0.49 (m, 2H), 0.33–0.29 (m, 2H). ^{13}C NMR (125 MHz, DMSO-d_6) δ 137.72, 135.96, 128.79, 128.50, 128.28, 127.99, 127.39, 127.31, 126.97, 124.72, 123.24, 59.73, 45.92, 9.18, 3.91. ESI-LRMS *m/z*: 365.0 [M − H]$^-$. ESI-HRMS calcd for $C_{21}H_{21}N_2O_2S$ [M − H]$^-$ 365.1329, found 365.1332.

4.1.31. N-benzyl-5-(cyclohexylamino)naphthalene-1-sulfonamide hydrochloride (*11v*)

Compound **11v** was prepared in a similar manner as described for compound **11u**. Yield: 68%. Mp 185–187 °C. ^{1}H NMR (500 MHz, DMSO-d_6) δ 8.61–8.55 (m, 1H), 8.51 (d, J = 8.6 Hz, 1H), 8.45–8.28 (m, 1H), 8.15 (d, J = 7.3 Hz, 1H), 7.67–7.58 (m, 2H), 7.51–7.31 (m, 1H), 7.19–7.04 (m, 5H), 4.03 (d, J = 6.1 Hz, 2H), 3.45 (tt, J = 11.2, 3.8 Hz, 1H), 2.01 (dd, J = 12.8, 3.8 Hz, 2H), 1.77 (dt, J = 13.3, 3.5 Hz, 2H), 1.62 (dt, J = 12.9, 3.5 Hz, 1H), 1.52 (q, J = 10.2 Hz, 2H), 1.29 (q, J = 12.6 Hz, 2H), 1.16 (qt, J = 12.6, 3.4 Hz, 1H). ^{13}C NMR (125 MHz, DMSO-d_6) δ 137.61, 136.30, 128.90, 128.77, 127.95, 127.78, 127.49, 127.41, 126.93, 125.65, 124.06, 56.53, 45.93, 30.43, 25.10, 24.37. ESI-LRMS *m/z*: 395.3 [M + H]$^+$. ESI-HRMS calcd for $C_{23}H_{27}N_2O_2S$ [M + H]$^+$ 395.1788, found 395.1791.

4.1.32. N-benzyl-5-(piperidin-4-ylamino)naphthalene-1-sulfonamide dihydrochloride (*11w*)

Compound **11w** was prepared in a similar manner as described for compound **11u**. Yield: 60%. Mp > 250 °C. ^{1}H NMR (500 MHz, DMSO-d_6) δ 9.24 (d, J = 11.1 Hz, 1H), 9.17–9.07 (m, 1H), 8.58 (d, J = 8.5 Hz, 1H), 8.41 (t, J = 6.2 Hz, 1H), 8.07 (d, J = 7.2 Hz, 1H), 7.92 (d, J = 8.5 Hz, 1H), 7.47 (dt, J = 12.1, 8.3 Hz, 2H), 7.25–7.14 (m, 5H), 6.82 (d, J = 7.8 Hz, 1H), 3.98 (d, J = 6.2 Hz, 2H), 3.78 (tt, J = 10.2, 3.6 Hz, 1H), 3.34 (dt, J = 12.8, 3.3 Hz, 2H), 3.04 (q, J = 11.6 Hz, 2H), 2.15 (dd, J = 14.2, 3.8 Hz, 2H), 1.91–1.79 (m, 2H). ^{13}C NMR (125 MHz, DMSO-d_6) δ 143.12, 137.89, 135.55, 129.07, 128.62, 128.22, 128.02, 127.77, 127.41, 126.98, 124.06, 122.08, 112.79, 105.43, 47.22, 45.91, 42.15, 27.90. ESI-LRMS *m/z*: 396.3 [M + H]$^+$. ESI-HRMS calcd for $C_{22}H_{26}N_3O_2S$ [M + H]$^+$ 396.1740, found 396.1744.

4.1.33. N-benzyl-5-((1-methylpiperidin-4-yl)amino)naphthalene-1-sulfonamide dihydrochloride (*11x*)

Compound **11x** was prepared in a similar manner as described for compound **11u**. Yield: 66%. Mp 159–160 °C. ^{1}H NMR (500 MHz, CD_3OD) δ 8.44 (d, J = 8.7 Hz, 1H), 8.37 (d, J = 8.5 Hz, 1H), 8.23 (dd, J = 7.4, 1.0 Hz, 1H), 7.66–7.59 (m, 2H), 7.35 (d, J = 7.6 Hz, 1H), 7.09–7.00 (m, 5H), 4.06 (s, 2H), 3.96 (tt, J = 11.3, 3.9 Hz, 1H), 3.67–3.62 (m, 2H), 3.18 (t, J = 12.4 Hz, 2H), 2.90 (s, 3H), 2.38 (d, J = 14.2 Hz, 2H), 2.20–2.08 (m, 2H). ^{13}C NMR (125 MHz, CD_3OD) δ 138.40, 137.97, 137.78, 130.91, 130.82, 129.11, 129.03, 128.74, 128.24, 127.70, 127.11, 125.62, 121.54, 115.66, 54.42, 52.74, 47.70, 43.79, 29.29. ESI-LRMS *m/z*: 408.1 [M − H]$^-$. ESI-HRMS calcd for $C_{23}H_{26}N_3O_2S$ [M − H]$^-$ 408.1751, found 408.1759.

4.1.34. N-benzyl-5-((1-ethylpiperidin-4-yl)amino)naphthalene-1-sulfonamide dihydrochloride (*11y*)

Compound **11y** was prepared in a similar manner as described for compound **11u**. Yield: 65%. Mp 192–194 °C. ^{1}H NMR (500 MHz, CD_3OD) δ 8.58 (d, J = 8.7 Hz, 1H), 8.37 (d, J = 8.6 Hz, 1H), 8.27 (dd, J = 7.3, 1.0 Hz, 1H), 7.71–7.65 (m, 2H), 7.51 (d, J = 7.6 Hz, 1H), 7.09–7.01 (m, 5H), 4.08 (s, 2H), 4.03–3.97 (m, 1H), 3.71 (d, J = 12.9 Hz, 2H), 3.21 (q, J = 7.3 Hz, 2H), 3.10 (td, J = 13.1, 2.7 Hz, 2H), 2.39 (d, J = 13.9 Hz, 2H), 2.22 (qd, J = 13.1, 3.9 Hz, 2H), 1.38 (t, J = 7.3 Hz, 3H). ^{13}C NMR (125 MHz, CD_3OD) δ 138.36, 135.69, 131.00, 130.93, 130.64, 129.12, 128.75, 128.25, 127.52, 127.42, 126.32, 124.96, 123.67, 118.31, 54.42, 53.30, 51.83, 47.71, 28.71, 9.74. ESI-LRMS *m/z*: 421.9 [M − H]$^-$. ESI-HRMS calcd for $C_{24}H_{28}N_3O_2S$ [M − H]$^-$ 422.1908, found 422.1917.

4.1.35. 5-((1-Acetylpiperidin-4-yl)amino)-N-benzylnaphthalene-1-sulfonamide hydrochloride (*11z*)

Compound **11z** was prepared in a similar manner as described for compound **11u**. Yield: 60%. Mp 162–163 °C. ^{1}H NMR (400 MHz, CD_3OD) δ 8.89 (d, J = 8.0 Hz, 1H), 8.37–8.29 (m, 2H), 7.84–7.74 (m, 3H), 7.05–6.96 (m, 5H), 4.67 (d, J = 13.1 Hz, 1H), 4.11 (s, 2H), 3.98 (tt, J = 11.6, 4.0 Hz, 1H), 3.67–3.64 (m, 1H), 3.23–3.11 (m, 1H), 2.67 (t, J = 12.2 Hz, 1H), 2.16 (s, 3H), 2.14–2.06 (m, 2H), 1.97–1.71 (m, 2H). ^{13}C NMR (125 MHz, CD_3OD) δ 171.84, 139.16, 138.21, 131.44, 130.87, 130.84, 129.07, 128.76, 128.50, 128.21, 128.19, 128.13, 127.83, 127.12, 124.58, 60.61, 47.67, 45.68, 41.00, 30.47, 29.79, 21.09. ESI-LRMS *m/z*: 438.4 [M + H]$^+$. ESI-HRMS calcd for $C_{24}H_{26}N_3O_3S$ [M + H]$^+$ 438.1846, found 438.1844.

4.1.36. 5-((1-Benzoylpiperidin-4-yl)amino)-N-benzylnaphthalene-1-sulfonamide hydrochloride (*11aa*)

Compound **11aa** was prepared in a similar manner as described for compound **11u**. Yield: 59%. Mp 258–260 °C. ^{1}H NMR (500 MHz, DMSO-d_6) δ 8.50 (d, J = 8.6 Hz, 1H), 8.36 (t, J = 6.3 Hz, 1H), 8.07 (d, J = 7.2 Hz, 1H), 7.89 (d, J = 8.5 Hz, 1H), 7.50–7.38 (m, 6H), 7.23–7.14 (m, 5H), 6.79 (d, J = 7.9 Hz, 1H), 6.10 (d, J = 7.5 Hz, 1H), 4.48 (s, 1H), 3.98 (d, J = 6.2 Hz, 2H), 3.86–3.76 (m, 1H), 3.72–3.58 (m, 1H), 3.30–3.19 (m, 1H), 3.12–2.97 (m, 1H), 2.19–1.94 (m, 2H), 1.63–1.48 (m, 2H). ^{13}C NMR (125 MHz, DMSO-d_6) δ 169.00, 143.63, 137.89, 136.34, 135.49, 129.41, 129.09, 128.74, 128.46, 128.21, 128.03, 127.48, 127.40, 126.98, 126.60, 123.92, 121.96, 112.12, 104.85, 49.20, 46.20, 45.91, 40.70, 31.74, 31.00. ESI-LRMS *m/z*: 498.0 [M − H]$^-$. ESI-HRMS calcd for $C_{29}H_{28}N_3O_3S$ [M − H]$^-$ 498.1857, found 498.1862.

4.1.37. Benzyl 4-((5-(N-benzylsulfamoyl)naphthalen-1-yl)amino) piperidine-1-carboxylate hydrochloride (*11 ab*)

Compound **11 ab** was prepared in a similar manner as described for compound **11u**. Yield: 62%. Mp 145–147 °C. ^{1}H NMR (400 MHz, DMSO-d_6) δ 8.52 (d, J = 8.6 Hz, 1H), 8.48 (d, J = 6.1 Hz, 1H), 8.16–8.14 (m, 1H), 8.11 (d, J = 7.2 Hz, 1H), 7.55 (td, J = 8.3, 3.5 Hz, 2H), 7.41–7.35 (m, 4H), 7.35–7.28 (m, 1H), 7.21–7.11 (m, 6H), 5.10 (s, 2H), 4.07 (d, J = 13.4 Hz, 2H), 4.00 (d, J = 6.0 Hz, 2H), 3.73 (tt, J = 10.2, 3.4 Hz, 1H), 2.98 (s, 2H), 2.02 (d, J = 10.6 Hz, 2H), 1.60 (q, J = 11.4 Hz, 2H). ^{13}C NMR (125 MHz, DMSO-d_6) δ 154.41, 137.77, 137.01, 135.93, 129.01, 128.51, 128.45, 128.25, 128.01, 127.84, 127.52, 127.42, 126.99, 124.81, 123.08, 66.20, 51.77, 45.92, 42.52, 30.28. ESI-LRMS *m/z*:

530.3 $[M + H]^+$. ESI-HRMS calcd for $C_{30}H_{32}N_3O_4S$ $[M + H]^+$ 530.2108, found 530.2118.

4.1.38. N-benzyl-5-((1-(methylsulfonyl)piperidin-4-yl)amino) naphthalene-1-sulfonamide hydrochloride (**11ac**)

Compound **11ac** was prepared in a similar manner as described for compound **11u**. Yield: 71%. Mp 159–161 °C. ^{1}H NMR (500 MHz, DMSO-d_6) δ 8.52 (d, J = 8.6 Hz, 1H), 8.43 (t, J = 6.3 Hz, 1H), 8.10 (dd, J = 7.3, 1.1 Hz, 1H), 8.04 (d, J = 8.6 Hz, 1H), 7.57–7.47 (m, 2H), 7.23–7.13 (m, 5H), 7.04–6.88 (m, 1H), 3.99 (d, J = 6.0 Hz, 2H), 3.69–3.59 (m, 3H), 2.93 (dd, J = 12.2, 2.6 Hz, 2H), 2.90 (s, 3H), 2.10 (dd, J = 13.5, 3.6 Hz, 2H), 1.71 (qd, J = 11.7, 4.0 Hz, 2H). ^{13}C NMR (125 MHz, DMSO-d_6) δ 137.80, 135.77, 129.03, 128.42, 128.38, 128.00, 127.53, 127.40, 126.97, 124.47, 122.63, 50.10, 45.91, 44.57, 34.48, 30.11. ESI-LRMS *m/z*: 472.1 $[M - H]^-$. ESI-HRMS calcd for $C_{23}H_{26}N_3O_4S_2$ $[M - H]^-$ 472.1370, found 472.1378.

4.2. Biological evaluation

4.2.1. HTS screening for NSD2 inhibitors

The compound library used in this study consisted of 296 080 compounds, synthetic and natural product-derived compounds solubilized in 100% DMSO prior to application in the HTS campaign. Recombinant human NSD2 (aa941-1240) was purchased from BPS Bioscience. The reaction was carried out in white 384-well plates (ProxiPlateTM-384 Plus, PerkinElmer), using AlphaLISA method. In brief, the assay were diluted in assay buffer (50 mM Tris-HCl, 0.01% Tween-20, 50 mM NaCl, 5 mM $MgCl_2$, 1 mM DTT, pH8.5) for 3 h at room temperature, containing 2 μL NSD2 enzyme solution (10 nM), 2 μL substrate (20 μM SAM, 0.15 ng/mL Nucleosomes) and 1 μL compound (20 μg/mL) or control (2% DMSO as positive control, SAH as negative control), followed by the addition of 2.5 μL High Salt buffer (50 mM Tris-HCl, 1 M NaCl, 0.1% Tween-20, 0.3% poly-L-lysine, pH7.4) to stop the reaction. The activity of NSD2 was detected by using AlphaLISA NSD2 Histone H3 Lysine-*N*-methyltransferase assay (PerkinElmer). The fluorescence intensity was measured with excitation and emission wavelengths at 680 and 615 nm using Envision (PerkinElmer). Hits identified from the primary screen were subsequently rescreened against NSD2 at two points (20 μg/mL and 2 μg/mL) in duplicate wells. And IC_{50} values were determined using the AlphaLISA assay described above. Selected hits were dissolved and serially diluted in 100% DMSO, with a final in-assay concentration of 2% DMSO in duplicate wells. The results were obtained using an Envision (PerkinElmer) and the IC_{50} data was calculated using the software GraphPad Prism 5, and chosen the equation "sigmoidal dose-response (variable slope)" for curve fitting.

4.2.2. NMR experiments

Ligand observed CPMG and saturation transfer difference (STD) NMR experiments were applied to investigate ligand-protein interactions. All NMR spectra were acquired at 25 °C on a Bruker Avance III 600 MHz NMR spectrometer equipped with a cryoprobe (Bruker biospin, Germany). Samples containing 200 mM compound **9c**, 200 mM compound **9c** in the presence of 4 μM NSD2 were dissolved in phosphate buffer (20 mM NaH_2PO_4, 20 mM Na_2HPO_4, 100 mM NaCl, 5% DMSO-d_6, pH 7.4) and then used in NMR data acquisition.

4.2.3. Selectivity assays

The selectivity of compound **9c** against NSD1, SETD2, DOT1L, PRMT4, PRMT5 was determined using AlphaLISA immunodetection assay as described previously. The selectivity against EZH2, MLL1, and MLL4 methylases were assessed with homogenous time-resolved fluorescence resonance energy transfer (HTRF) assays. Dilute enzyme, SAM(S-(5′-Adenosyl)-L-methionine chloride), compounds and peptide substrate in Assay Buffer just before use. Add 4 μL of inhibitor, 2 μL of enzyme to the wells of a white OptiPlate-384 and incubate for 10 min at room temperature. Subsequently, add 4 μL of peptide/SAM mix to the reaction system. Cover the plate with TopSeal-A film and incubate at room temperature for 4 h. Prepare a 2X mix of antibody and SA-XL665,respectively, in Detection Buffer. Add 10 μL of detection mixture (2X) to the plate. Cover with TopSeal-A film and incubate in subdued light for 1 h at room temperature. Remove plate sealer and read fluorescence emission at 665 nm and 620 nm wavelengths on an HTRF compatible reader. The resultant data were analyzed with GraphPad Prism.

4.2.4. Cell lines

The human B cell precursor leukemia cell line RS4:11, OPM-2 and human myeloma cell line KMS11 were cultured in the altered RPMI-1640 medium (Invitrogen) containing 10% selected FBS (Gibco) and 2 mM Glutamine. The MV4:11 cell line was maintained in IMDM (Iscove's Modified Dulbecco's Medium) supplemented with 10% selected FBS (Gibco).

4.2.5. Western blot analysis

The cells were lysed in buffer containing 2% SDS and quantified by performing a BCA assay. An equal amount of protein was subjected to electrophoresis on SDS–PAGE and transferred to nitrocellulose membranes, incubated with primary antibodies and then incubated with horseradish peroxidase-conjugated secondary antibodies. Primary antibodies used were as follows: anti-beta-actin (Proteintech Group, 66 009-1-lg), anti-histone H3 (Cell Signaling Technology, #9715), anti-WHSC1/NSD2 (abcam, ab75359),anti-Di-Methyl-Histone H3 (Lys27) (Cell Signaling Technology, #9728), anti-Tri-Methyl-Histone H3 (Lys27) (Cell Signaling Technology, #9733), anti-Tri-Methyl-Histone H3 (Lys36) (Cell Signaling Technology, #4909), anti-Di-Methyl-Histone H3 (Lys36) (Cell Signaling Technology, #2901), anti-Di-Methyl-Histone H3 (Lys4) (Cell Signaling Technology, #9725), anti-Di-Methyl-Histone H3 (Lys9) (Cell Signaling Technology, #4658), anti-Tri-Methyl-Histone H3 (Lys79) (Cell Signaling Technology, #4260). The detection was performed using a SuperSignal west pico stable peroxide solution (Thermo Fisher Scientific).

4.2.6. Cell proliferation assay

Cells were seeded in 96-well plates at 6000–20000 cells per well in triplicate for 24 h. Then the cells were treated with increasing doses of compound **9c** and were cultured for another 6 d. Cell viability was examined using the cell counting kit-8 (Life Technologies) according to the manufacturer's instructions. The optical density measured at a wavelength of 450 nm was used as an indicator of cell viability.

4.2.7. Cell cycle analysis and annexin V staining

Cell cycle analysis was conducted by incorporating propidium iodide (PI). Leukemic cells were treated with indicated does of compound **9c** for 72 h. Then cells were washed twice and fixed by 70% pre-cooled ethanol overnight. Cells were resuspended in stain buffer containing 5 μg/mL ribonuclease A (Sigma-Aldrich) and 5 μg/mL PI for 45 min in room tempreture. Acquisition was performed on FACSCanto (BD Biosciences), and results were analyzed using modifit software.

For apoptosis assay, 10^5 cells were collected and re-suspended in 100 μL annexin V binding solution containing 0.25 μg/mL anti-annexin V-FITC and 1 μg/mL PI in the dark for 15 min. Samples were diluted with 400 μL annexin V binding solution and analyzed with the FACS.

4.2.8. RNA-seq

RNA-seq data was generated by novogene. RS4:11 cells plated in 10 cm dishes were treated with DMSO or 10 μM compound **9c** for 6 days respectively. Then cells were washed by PBS for 3 times and then lysed by trizol at room temperature. Samples were sent to novogene on dry ice. A total amount of 3 mg RNA per sample was used as input material for the RNA sample preparations. Sequencing libraries were generated using NEBNext UltraTM RNA library prep it for illumina (NEB, USA) following manufacturer's recommendations and index codes were added to attribute sequences to each sample. The clustering of the index-coded samples was performed on a cBot cluster generation system using TruSeq PE cluster kit v3-cBot-HS (Illumia) according to the manufacturer's instructions. After cluster generation, the library preparations were sequenced on an illumina platform and 125 bp/150 bp paired-end reads were generated. GO was used for cellular pathway analysis.

4.2.9. ChIP-qPCR

ChIP-qPCR assay was performed using SimpleChIP plus enzymatic chromatin IP kit (Magnetic Beads) (Cell Signaling Technology, #9005) according to the procedures provided by the manufacturer. Antibodies used for ChIP were as follows: anti-immunoglobulin G (Cell Signaling Technology, #2729), anti-Histone H3 (Cell Signaling Technology, #4620), anti-Histone H3K36me2 (Invitrogen, # MA5-14867). Purified DNA was subject to quantitative real-time PCR analysis, using primers that encompass genes' promoter region. All samples were normalized to input as control. The sequences of the primers were as follows:

***TGFA* promoter**:
5′-GGAGCTCACGGACTGACC-3'
5′-GATCTACCCGGAGCACGTAG-3'
***TGFA* TSS**:
5′-CGTAGCCGGATTGTCCTG-3'
5′-GCCCCTCGGTGTAGGTAAC-3'
***TGFA* (1) 6 kb**:
5′-CAAGATGAAAACAGGTGAAGC A-3'
5′-TCAAGACGGAACCCCTTTAG-3'
***TGFA* (2) 22 kb**:
5′-GTTGAAAGCGACGAAACCAT-3'
5′-GTGCTGGTTTGGGTTTTCTC-3'
***TGFA* (3) 57 kb**:
5′-CTGGAAAAACTGGGGAAAGA-3'
5′-TTCTAGGCTTTGCACTTGCTC-3'
***TGFA* (4) 73 kb**:
5′-TCCTGCCTCTTCCATGATCT-3'
5′-AAACCAGGAATTCCCAACTTTT-3'
***TGFA* (5) 101 kb**:
5′-AGAGGTGAGTAACTTGTCAAAGGTC-3'
5′-GTAGGGACCCCTTACATCCTG-3'
PAK1 promoter:
5′-TGTTTTCTTTCTGTGGGAGAGG-3'
5′-CACATTAGTTCAAACATCTCCGTTA-3'
PAK1 TSS:
5′-GAGGGGGCGTCTACTGTG-3'
5′-GTACAATAGCGCGGCTGTG-3'
PAK1 (1) 7 kb:
5′-CACCCCCATTTCAAGTGC-3'
5′-TAAGTGCAAGTGCCATGTGAA-3'
PAK1 (2) 47 kb:
5′-CAGAACAAGAAAAGTTCAAGATGC-3'
5′-ATCCCACTACCAACCCCATT-3'
PAK1 (3) 90 kb:
5′-CCAGATTCACAAAGCACATGA-3'
5′-TCCCTCAGTCCGAAGCTCT-3'
PAK1 (4) 124 kb:
5′-TTTCCTGTTCCTGCTTGCTT-3'
5′-AATTAGAGCCACGTGCCAAG-3'
***MET* promoter**:
5′-GGAGACTCGGTCCCGCTTAT-3'
5′-CCCAGCTCAGGCAGTCTGA-3'
***MET* TSS**:
5′-TGACACTCGCCTCCCAAG-3'
5′-AAGTTAGCACAGCCGGAGATA-3'
***MET* (1) 3 kb**:
5′-CGTTTCTTCTTTAGGCATTAGGC-3'
5′-ACCACGGAAAAGAAAGCGTA-3'
***MET* (2) 26 kb**:
5′-TGGTGCAGAGGAGCAATGG-3'
5′-CCCAGTCTTGTACTCAGCAAC-3'
***MET* (3) 45 kb**:
5′-GTCATCACCACGAGGCTGT-3'
5′-GTGATTCACAAGGTGATGGAAG-3'
***MET* (4) 71 kb**:
5′-GCTCGCAGCAAGATCAGTG-3'
5′-CCGTGTACCTCTGTTGGACA-3'
***MET* (5) 114 kb**:
5′-GGAGAAATTGGATGCTCAACA-3'
5′-TTCCAAGACCCTTCTGGTGT-3'
RRAS2 promoter:
5′-AGTGGGTGTCAGTTGGGAGT-3'
5′-CCACACAATCCCTTACATAGACAA-3'
RRAS2 TSS:
5′-CCAAGTTGCCACCGCTAT-3'
5′-AGCCGGGCTTTACTGCTC-3'
RRAS2 (1) 5 kb:
5′-CAAATCTCCTGAAATCTCTTCTCG-3'
5′-TGCTGAGTACTTTTTCATTGCTTT-3'
RRAS2 (2) 15 kb:
5′-CACGCCTGTACTCCCAGTTAC-3'
5′-TGTCCCCGGCTTAAGTGAT-3'
RRAS2 (3) 24 kb:
5′-GGTCCTTGCCATCAACAACT-3'
5′-TGAGGAAAAAGCTAGTACAATAGGG-3'
RRAS2 (4) 50 kb:
5′-AATGTGCCAAGCATTGTGTC-3'
5′-GAAACTGCCAGCCCTCTAAG-3'
RRAS2 (5) 74 kb:
5′-CCATACCAATTCAAGTATGGTTTAAGA-3'
5′-GGGACTTTAGGCATACACCACT-3'

4.2.10. Tumor xenograft experiment

RS4:11 cells at a density of 1×10^7 in 0.2 mL of phosphate-buffered saline were injected subcutaneously into the flank of 4-week-old SCID female mice. When the tumor volume reached approximately 100 mm^3, mice were distributed into three groups ($n = 8$ per group) and treated with 25 mg/kg compound **9c**, 50 mg/kg compound **9c** or vehicle by intravenous and intraperitoneal injection every day. The tumors and body weight of the mice were measured individually twice weekly. This study was conducted in strict accordance with the recommendations in the guide for the care and use of laboratory animals.

4.2.11. Statistical analysis

Meaningful differences and changes were performed using student's *t*-test with Graphpad prism 6 software. Results and averaged data are presented as mean ± standard deviation (SD). When $P < 0.05$, results were considered as statistically significant.

4.2.12. Pharmacokinetic profiles in CD-1 mice

Compound **9c** (PEG300/EtOH/NaCl = 40/10/50, v/v/v) was

subjected to PK studies in CD-1 mice. Compound **9c** was administered *via* the intraperitoneal and intravenous route at 2 mg/kg in CD-1 mice, respectively. After administration, blood samples were orderly collected at 0 h, 0.083 h, 0.25 h, 0.5 h, 1 h, 2 h, 4 h, 6 h, 8 h, and 24 h. The blood samples were centrifuged at 11 000 rpm for 5 min to obtain the plasma fraction and added PK-IS immediately. The plasma samples were deproteinized with methanol and acetonitrile (1:1, v/v). After centrifugation, the supernatant was diluted with acetonitrile and water. The compound concentrations in the supernatant were measured by LC/MS/MS.

Declaration of competing interest

The authors declare that they have no known competing financial interests or personal relationships that could have appeared to influence the work reported in this paper.

Acknowledgement

We are grateful for the National Natural Science Foundation of China (Grant 21922707, 21632008, 21877118, 81620108027, 81821005 and 91953108), the Major projects of National Natural Science Foundation of China (Grant 81991523), the Collaborative Innovation Cluster Project of Shanghai Municipal Commission of Health and Family Planning (Grant 2019CXJQ02), the Science and Technology Commission of Shanghai Municipality (Grant 18JC1411304, 19430750100, and 18431907100).

Appendix A. Supplementary data

Supplementary data to this article can be found online at https://doi.org/10.1016/j.ejmech.2021.113592.

References

[1] M. Morishita, D. Mevius, E. di Luccio, In vitro histone lysine methylation by NSD1, NSD2/MMSET/WHSC1 and NSD3/WHSC1L, BMC Struct. Biol. 14 (2014) 25.
[2] M. Morishita, E. di Luccio, Cancers and the NSD family of histone lysine methyltransferases, Biochim. Biophys. Acta 1816 (2011) 158–163.
[3] I. tec, T.J. Wright, G.J. van Ommen, P.A. de Boer, A. van Haeringen, A.F. Moorman, M.R. Altherr, J.T. den Dunnen, WHSC1, a 90 kb SET domain-containing gene, expressed in early development and homologous to a Drosophila dysmorphy gene maps in the Wolf-Hirschhorn syndrome critical region and is fused to IgH in t(4;14) multiple myeloma, Hum. Mol. Genet. 7 (1998) 1071–1082.
[4] T. Vougiouklakis, R. Hamamoto, Y. Nakamura, V. Saloura, The NSD family of protein methyltransferases in human cancer, Epigenomics 7 (2015) 863–874.
[5] N.P. Coussens, S.C. Kales, M.J. Henderson, O.W. Lee, K.Y. Horiuchi, Y. Wang, Q. Chen, E. Kuznetsova, J. Wu, S. Chakka, D.M. Cheff, K.C. Cheng, P. Shinn, K.R. Brimacombe, M. Shen, A. Simeonov, M. Lal-Nag, H. Ma, A. Jadhav, M.D. Hall, High-throughput screening with nucleosome substrate identifies small-molecule inhibitors of the human histone lysine methyltransferase NSD2, J. Biol. Chem. 293 (2018) 13750–13765.
[6] Y. Li, P. Trojer, C.F. Xu, P. Cheung, A. Kuo, W.J. Drury 3rd, Q. Qiao, T.A. Neubert, R.M. Xu, O. Gozani, D. Reinberg, The target of the NSD family of histone lysine methyltransferases depends on the nature of the substrate, J. Biol. Chem. 284 (2009) 34283–34295.
[7] Q. Qiao, Y. Li, Z. Chen, M. Wang, D. Reinberg, R.M. Xu, The structure of NSD1 reveals an autoregulatory mechanism underlying histone H3K36 methylation, J. Biol. Chem. 286 (2011) 8361–8368.
[8] K. Nimura, K. Ura, H. Shiratori, M. Ikawa, M. Okabe, R.J. Schwartz, Y. Kaneda, A histone H3 lysine 36 trimethyltransferase links Nkx2-5 to Wolf-Hirschhorn syndrome, Nature 460 (2009) 287–291.
[9] E. Martinez-Garcia, R. Popovic, D.J. Min, S.M. Sweet, P.M. Thomas, L. Zamdborg, A. Heffner, C. Will, L. Lamy, L.M. Staudt, D.L. Levens, N.L. Kelleher, J.D. Licht, The MMSET histone methyl transferase switches global histone methylation and alters gene expression in t(4;14) multiple myeloma cells, Blood 117 (2011) 211–220.
[10] J.D. Jaffe, Y. Wang, H.M. Chan, J. Zhang, R. Huether, G.V. Kryukov, H.E. Bhang, J.E. Taylor, M. Hu, N.P. Englund, F. Yan, Z. Wang, E. Robert McDonald 3rd, L. Wei, J. Ma, J. Easton, Z. Yu, R. deBeaumount, V. Gibaja, K. Venkatesan, R. Schlegel, W.R. Sellers, N. Keen, J. Liu, G. Caponigro, J. Barretina, V.G. Cooke, C. Mullighan, S.A. Carr, J.R. Downing, L.A. Garraway, F. Stegmeier, Global chromatin profiling reveals NSD2 mutations in pediatric acute lymphoblastic leukemia, Nat. Genet. 45 (2013) 1386–1391.
[11] M. Morishita, D. Mevius, E. di Luccio, In vitro histone lysine methylation by NSD1, NSD2/MMSET/WHSC1 and NSD3/WHSC1L, BMC Struct. Biol. 14 (2014) 25.
[12] D.J. Min, T. Ezponda, M.K. Kim, C.M. Will, E. Martinez-Garcia, R. Popovic, V. Basrur, K.S. Elenitoba-Johnson, J.D. Licht, MMSET stimulates myeloma cell growth through microRNA-mediated modulation of c-MYC, Leukemia 27 (2013) 686–694.
[13] T. Ezponda, R. Popovic, M.Y. Shah, E. Martinez-Garcia, Y. Zheng, D.J. Min, C. Will, A. Neri, N.L. Kelleher, J. Yu, J.D. Licht, The histone methyltransferase MMSET/WHSC1 activates TWIST1 to promote an epithelial-mesenchymal transition and invasive properties of prostate cancer, Oncogene 32 (2013) 2882–2890.
[14] V. Saloura, H.S. Cho, K. Kiyotani, H. Alachkar, Z. Zuo, M. Nakakido, T. Tsunoda, T. Seiwert, M. Lingen, J. Licht, Y. Nakamura, R. Hamamoto, WHSC1 promotes oncogenesis through regulation of NIMA-related kinase-7 in squamous cell carcinoma of the head and neck, Mol. Canc. Res. 13 (2015) 293–304.
[15] G. Toyokawa, H.S. Cho, K. Masuda, Y. Yamane, M. Yoshimatsu, S. Hayami, M. Takawa, Y. Iwai, Y. Daigo, E. Tsuchiya, T. Tsunoda, H.I. Field, J.D. Kelly, D.E. Neal, Y. Maehara, B.A.J. Ponder, Y. Nakamura, R. Hamamoto, Histone lysine methyltransferase wolf-Hirschhorn syndrome candidate 1 is involved in human carcinogenesis through regulation of the wnt pathway, Neoplasia 13 (2011) 887.
[16] P. Yang, L. Guo, Z.J. Duan, C.G. Tepper, L. Xue, X. Chen, H.J. Kung, A.C. Gao, J.X. Zou, H.W. Chen, Histone methyltransferase NSD2/MMSET mediates constitutive NF-kappaB signaling for cancer cell proliferation, survival, and tumor growth via a feed-forward loop, Mol. Cell Biol. 32 (2012) 3121–3131.
[17] I.A. Asangani, B. Ateeq, Q. Cao, L. Dodson, M. Pandhi, L.P. Kunju, R. Mehra, R.J. Lonigro, J. Siddiqui, N. Palanisamy, Y.M. Wu, X. Cao, J.H. Kim, M. Zhao, Z.S. Qin, M.K. Iyer, C.A. Maher, C. Kumar-Sinha, S. Varambally, A.M. Chinnaiyan, Characterization of the EZH2-MMSET histone methyltransferase regulatory axis in cancer, Mol. Cell. 49 (2013) 80–93.
[18] D. Tisi, E. Chiarparin, E. Tamanini, P. Pathuri, J.E. Coyle, A. Hold, F.P. Holding, N. Amin, A.C. Martin, S.J. Rich, V. Berdini, J. Yon, P. Acklam, R. Burke, L. Drouin, J.E. Harmer, F. Jeganathan, R.L. van Montfort, Y. Newbatt, M. Tortorici, M. Westlake, A. Wood, S. Hoelder, T.D. Heightman, Structure of the epigenetic oncogene MMSET and inhibition by *N*-alkyl sinefungin derivatives, ACS Chem. Biol. 11 (2016) 3093–3105.
[19] M. Morishita, D.E.H.F. Mevius, Y. Shen, S. Zhao, E. di Luccio, BIX-01294 inhibits oncoproteins NSD1, NSD2 and NSD3, Med. Chem. Res. 26 (2017) 2038–2047.
[20] E. di Luccio, Inhibition of nuclear receptor binding SET domain 2/multiple myeloma SET domain by LEM-06 implication for epigenetic cancer therapies, J. Cancer Prev 20 (2015) 113.
[21] J. Baell, M.A. Walters, Chemistry: chemical con artists foil drug discovery, Nature 513 (2014) 481–483.
[22] X. Zhang, X.L. Zheng, H. Yang, J. Yan, X.H. Fu, R.R. Wei, X.W. Xu, Z.Q. Zhang, A.S. Yu, K.X. Zhou, J. Ding, M.Y. Geng, X. Huang, Piribedil disrupts the MLL1-WDR5 interaction and sensitizes MLL-rearranged acute myeloid leukemia (AML) to doxorubicin-induced apoptosis, Canc. Lett. 431 (2018) 150–156.
[23] A.J. Kuo, P. Cheung, K. Chen, B.M. Zee, M. Kioi, J. Lauring, Y. Xi, B.H. Park, X. Shi, B.A. Garcia, W. Li, O. Gozani, NSD2 links the dimethylation of histone H3 at lysine 36 to oncogenic programming, Mol. Cell. 44 (2011) 609.
[24] R. Stein, M.R. Smith, S. Chen, M. Zalath, D.M. Goldenberg, Goldenberg, Combining milatuzumab with bortezomib, doxorubicin, or dexamethasone improves responses in multiple myeloma cell lines, Clin. Canc. Res. 15 (2009) 2808–2817.